Office of Naval Research

Contract Nonr. 736(000) Project Nr. 330-027

Technical Report No. 10

August 20, 1954

Particle Size Determination of Spherical Colloidal Particles by Light Scattering

I. The Specific Turbidity

by

Richard M. Tabibian

Submitted By

W. Heller, Project Director

Chemistry Department, Wayne University

Detroit, Michigan

Office of Naval Research

Contract Nonr. 736(000) Project Nr. 330-027

Research on the Size and Shape of
Large Molecules and Colloidal
Particles

Technical Report No. 10

Particle Size Determination of Spherical Colloidal Particles by Light Scattering

I. The Specific Turbidity

by

Richard M. Tabibian

Submitted By

W. Heller, Project Director

Chemistry Department, Wayne University

Detroit, Michigan

August 20, 1954

Introductory Remarks

The present report is a greatly expanded version of the Master thesis submitted by R. M. Tahibian to the Graduate School of Wayne University, about one half year ago. The additional material contained in this version is a fraction of the work to be used towards the Ph.D. degree. It was decided to incorporate this material in order to bring, in one single report, the entire story of specific turbidity measurements, which, except for occasional additions, had been completed several months ago. An extract with the most essential findings was given in Technical Report 8.

W. Heller

CHAPTER I

INTRODUCTION

The technique of light scattering as a means of obtaining the molecular weight and dimensions of macromolecules and colloidal particles has been extensively exploited during the past decade. The tremendous increase in the large scale production of synthetic polymers and the expanding use of naturally occurring polymeric substances has produced a need for the rapid and simple determination of molecular weights and dimensions. In so far as the physical properties of these materials depend upon the size and shape of their constituent molecules, knowledge of these factors is of great importance.

Other methods of obtaining this information include those of osmotic pressure, viscosity, the ultracentrifuge techniques of sedimentation rate and sedimentation equilibrium, birefringence measurements, and electron microscopy. Light scattering offers certain advantages over these in that the method is sensitive to small changes and measurements can be simply and rapidly carried out. Furthermore, this method can be applied not only to sols but also to emulsions and aerosols which are not readily amenable to many of the above techniques. One further advantage is that one can follow rapid changes in the system without affecting the particles

during the measurements.

Light scattering as a means of determining particle sizes and molecular weights is well established for those particles whose dimensions are less than 1/10 the wave length of the incident light. In such cases the classical light scattering equations of Lord Rayleigh[1] and the equations of Einstein,[2] Smoluchowski,[3] Gans,[4] and Debye[5] are valid. However, for particles any one of whose dimensions exceeds 1/10 the wave length of the light, these equations become inapplicable. The rather complicated theoretical problem in the case of these larger particles was solved by Mie.[6]

This report describes a method for determining the size of colloidal particles whose dimensions are of the order of the wave length of light, i.e. greater than 1/10 λ. The preliminary work was carried out by Epel.[7] The objective here is to extend the data to include larger particle sizes and to make the previously obtained curve more secure. Monodisperse polystyrene and polyvinyltoluene latices provided by

---

[1]Rayleigh, Phil. Mag., 41, 447 (1871).

[2]Einstein, A., Ann. Physik, 33, 1275 (1910).

[3]Smoluchowski, M., Ann. Physik, 25, 205 (1908).

[4]Gans, R., Zeit. f. Physik, 17, 371 (1923).

[5]Debye, P., J. Appl. Physics, 15, 338 (1944).

[6]Mie, G., Ann. Physik, 25, 377 (1908).

[7]Epel, J., Light Scattering Methods for Determining the Size of Large Colloidal Particles, Dissertation, Wayne University (1951).

the Dow Chemical Company were used in this work. Finally, the experimental data are compared with the theoretical values obtained from the Mie equations by Pangonis and Heller[8] for values of the refractive ratio which correspond to that of the experimental system.

---

[8]Pangonis, W., Light Scattering by Colloidal Systems, Dissertation, Wayne University (1952).

CHAPTER II

REVIEW OF LIGHT SCATTERING METHODS

When a beam of light falls upon a system of particles differing with respect to refractive index from the medium in which they are suspended, the electric field associated with the light induces periodic oscillations of electrostatic charges in the material. The dispersed units of this material behave like oscillating dipoles or multipoles depending upon their size and act as secondary emitters of light.

The intensity, angular distribution, and state of polarization of the scattered radiation are determined by the size, shape, optical constants, and interactions of the particles in the scattering system.

A. Small Particles

The quantitative treatment of light scattering was first carried out by Lord Rayleigh[1] who investigated the case of small isotropic spheres (diameter less than $1/10\,\lambda$). Such particles may be considered as equivalent to oscillating dipoles. Hence, the electromagnetic field around the particle and the intensity of the scattered light can be calculated rather easily. The latter may be written in the form first

---

[1] Rayleigh, Phil. Mag., 41, 447 (1871).

given by Rayleigh.

$$J_\theta = I_o \frac{9\pi^2 V^2}{2\lambda^4 r^2} \left(\frac{m^2 - 1}{m^2 + 2} \right)^2 (1 + \cos^2 \theta) \qquad (1)$$

where

J_θ = intensity of light scattered at an angle θ by a single particle;

θ = angle of observation measured from the direction of propagation;

I_o = intensity of incident light;

λ = wave length of the incident light in the medium;

m = ratio of the refractive index of the particle, n_p, to that of the dispersing medium, n_o;

r = distance from the scattering particle to the observer;

V = volume of scattering particle.

Equation (1) applies to natural incident light.

Figure 1 is a radiation diagram of a single scattering particle. It shows the angular distribution of intensities in polar coordinates. The scattering particle is at the origin and the length of the line drawn from the origin to the curve is proportional to the intensity of the scattered light.

The scattered light can be considered as consisting of two incoherent linearly polarized components vibrating in orthoganol planes (dotted lines in Figure 1). The $\cos^2 \theta$ term of equation (1) refers to one component and the unity

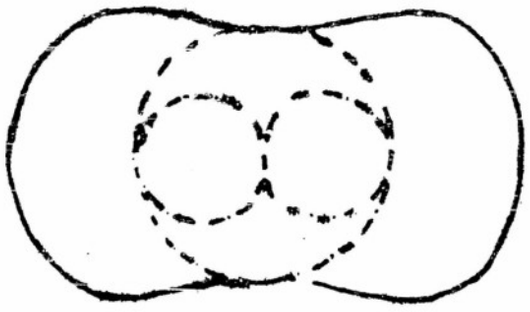

Fig. 1. Radiation Diagram of a Small Sphere.

term to the other. The total intensity of the light scattered at a given angle is the sum of the two components (solid line). One can see from the diagram that the same amount of light is scattered in the forward as in the backward direction and that the light scattered at 90° is perfectly plane polarized.

For a system containing many scattering particles, the total effect is a simple sum of the individual effects provided the system is dilute enough not to show any interference. The intensity of a beam of light in passing through such a scattering solution is decreased due to the loss of energy. For a non-absorbing system the fractional decrease in the intensity of the primary beam is proportional to the distance traversed, i.e.

$$\frac{dI}{I} = -\tau\, dl \qquad (2)$$

where l is the distance in cm. and I is the intensity, and

where the proportionality constant τ is called the turbidity. From equation (2) it follows that

$$\tau = \frac{\ln I_o/I}{l} \qquad (3)$$

Here I_o is the intensity of the incident light and I the intensity of the beam after traversing a distance l.

Equation (3) can be put into another form by the following considerations. Obviously, the loss of intensity $I_o - I$ is equal to the total light scattered, $I_s l$, where I_s is the light scattered per cm. The turbidity of a scattering system one cm. in thickness can then be expressed as

$$\tau = -\ln \frac{I_o - I_s}{I_o} = -\ln (1 - I_s/I_o) \qquad (4)$$

When the ratio I_s/I_o is very small (4) reduces to

$$\tau = I_s/I_o \qquad (5)$$

Hence, the turbidity per cm. is given by the ratio of the total scattered intensity to the intensity of the incident light.

Smoluchowski[2] and Einstein[3] have approached the matter of light scattering from a different viewpoint. In order to explain the scattering for pure liquids Smoluchowski considered spontaneous fluctuations in the density. These local

---

[2]Smoluchowski, M., Ann. Physik, 25, 208 (1908).

[3]Einstein, A., Ann. Physik, 33, 1275 (1910).

fluctuations produce inhomogeneities of the dielectric constant and these in turn behave as scattering centers. Einstein extended Smoluchowski's theory and included two component liquid mixtures in which he considered fluctuations in the concentration of one component with respect to the other. His development compares the thermal energy and the work necessary to produce such changes by an external pressure, P, and relates them through a probability function. He showed that the total light scattered by such a solution is proportional to

$$\frac{RT}{N\lambda^4} \cdot \frac{\left(c\frac{\partial \epsilon}{\partial c}\right)^2}{c\frac{\partial P}{\partial c}}$$

where ϵ is the dielectric constant of the solution, c the concentration, and N is Avogadro's number. The constant of proportionality was shown to be $8\pi^3/3$, so that from equation (5)

$$\tau = \frac{8\pi^3}{3\lambda^4 N} \cdot RT \cdot \frac{\left(c\frac{\partial \epsilon}{\partial c}\right)^2}{c\frac{\partial P}{\partial c}} \qquad (6)$$

when the incident light is of unit intensity.

Debye[4] interpreted the pressure term as osmotic pressure. For ideal solutions then $\partial P/\partial c$ is equal to RT/M from Van't Hoff's law, and replacing ϵ by n^2 the turbidity becomes

---

[4]Debye, P., J. App. Physics, 15, 338 (1944).

$$\tau = \frac{32\pi^3 Mc\, n_o^2}{3\lambda^4 N} \left(\frac{n_p - n_o}{c}\right)^2 \qquad (7)$$

This same expression can be obtained from the Rayleigh equation. Another form of the latter is

$$I_\theta = I_o \frac{8\pi^4 \nu \alpha^2}{\lambda^4 r^2} (1 + \cos^2 \theta) \qquad (8)$$

in which ν is the number of particles per cc., α is the polarizability of the particles, and the other symbols are as previously defined. The total light scattered is found by integrating (8) over the surface of a sphere.

$$I_s = \int_o^\pi I_\theta\, 2\pi r^2 \sin\theta\, d\theta \qquad (9a)$$

which yields

$$I_s = \frac{128}{3} \frac{I_o \pi^5 \nu \alpha^2}{\lambda^4} \qquad (9b)$$

Substituting this into equation (5) we get

$$\tau = \frac{128}{3} \frac{\pi^5 \nu \alpha^2}{\lambda^4} . \qquad (10)$$

The polarizability can be correlated with the refractive index by the expression

$$4\pi\nu\alpha = n_p^2 - n_o^2 = (n_p - n_o)(n_p + n_o). \qquad (11)$$

If n_p and n_o do not differ greatly, we can make the simplifying assumption that

$$4\pi\nu\alpha = (n_p - n_o)\,2n_o \qquad (12a)$$

from which

$$\alpha = \frac{n_o(n_p - n_o)}{2\pi\nu} \qquad (12b)$$

The insertion of this expression into (10) gives

$$\tau = \frac{32\pi^3}{3\lambda^4\nu}\, n_o^2 (n_p - n_o)^2 \qquad (13)$$

The quantity ν can be expressed in terms of weight concentration, c as

$$\nu = \frac{Nc}{M} \qquad (14)$$

where N is Avogadro's number and M is the molecular weight of the solute. The turbidity then becomes

$$\tau = \frac{32\pi^3 Mc}{3\lambda^4 N}\, n_o^2 \left(\frac{n_p - n_o}{c}\right)^2 \qquad (7)$$

which is identical with equation (7).

In the case of non-ideal solutions Doty and Zimm have found it necessary to express the osmotic pressure in terms of the modified Van't Hoff equation

$$P = \frac{cRT}{M} + Bc^2.$$

Substituting this into equation (6) they obtained the expression

$$H\frac{c}{\tau} = \frac{1}{M} + \frac{2Bc}{RT} \qquad (15)$$

where $H = \frac{32\pi^3 n_o^2}{3\lambda^4 N} \left(\frac{n_p - n_o}{c} \right)^2$.

By plotting $H\,c/\tau$ vs. c a straight line is obtained whose intercept is the reciprocal of the molecular weight. In this way the molecular weight of several polymers have been determined.

B. Large Particles with Refractive Ratio Near Unity.

All that precedes applies to particles whose dimensions are small compared to the wave length of visible light. In the case of larger particles it is no longer justifiable to represent the radiation as that of a single oscillating dipole. Each particle may now be considered as an assembly of oscillating dipoles. These induced dipoles are not in phase with each other and the radiation field at a distant point will be made up of a superposition of waves coming from different parts of the particle and interfering with each other. In addition, there is a distortion of the external field but for particles with a refractive ratio near unity this effect can be neglected.

The problem is then purely a geometrical task involving the tabulation of the decreased intensity of scattered light that will result for the interference of rays from every pair of volume elements in the scattering particle for every value of the angle Θ. This is identical mathematically with the

analogous problem previously studied by Debye[5] of X-ray and electron scattering by molecules. In this case the intensity calculated from the Rayleigh equation must be corrected by the factor

$$\sum_i \sum_j \frac{\sin\left[\frac{4\pi r_{ij}}{\lambda} \sin\frac{\theta}{2}\right]}{\frac{4\pi r_{ij}}{\lambda} \sin\frac{\theta}{2}}$$

where the double summation extends over all pairs of scattering elements i and j with r_{ij} being the distance between the ith and jth scattering element.

The distribution of the scattering elements can be expressed in terms of the vector distance between the separate elements and the probability density of distribution. Then for a given particle shape this factor can be replaced by its integral representation. For the particular case of spherical particles of diameter D this scattering factor becomes

$$\left[\frac{3}{x^3}(\sin x - x\cos x)\right]^2$$

where $x = \frac{2\pi D}{\lambda} \sin\frac{\theta}{2}$.

A plot of this factor shows that more light is now scattered in the forward than in the backward direction. This arises from the fact that the wavelets from particles along

---

[5] Debye, P., Ann. Physik, 46, 809 (1915).

the incident beam will be approximately in phase, but in the backward direction they will generally be out of phase with some destructive interference and a consequent loss in intensity. The larger the particle the greater will be the ratio of forward to backward scattering. Debye has pointed out that the ratio of the intensity of light scattered at two equal angles about the normal to the incident beam could be used as a criterion of particle size. This dissymmetry method, as it is called, has been used by a number of investigators[6-9] to determine the size and shape of various particles.

C. Particles of any Size and Refractive Ratio.

When the size of the scattering particle is sufficiently large and the refractive ratio significantly greater than unity, the distortion of the external field brought about by its interaction with the internal field can no longer be neglected. Furthermore, the tacit assumption that the oscillating dipoles emit independently of each other becomes invalid.

---

[6]Doty, P., Affens, W. A., and Zimm, B. H., Trans. Faraday Soc., 42B, 66 (1946).

[7]Oster, G., Doty, P. M., and Zimm, B. H., J. Am. Chem. Soc., 69, 1193 (1947).

[8]Doty, P. M., and Steiner, R., J. Chem. Phys., 18, 1211 (1950).

[9]Debye, P. and Annacker, E. W., J. Phys. and Coll. Chem., 55, 644 (1951).

The solution of this problem can be obtained by solving the boundary value problem of a plane wave incident upon a particle of arbitrary size, shape, orientation, and index of refraction. This general case is prohibitive because of its complexity but the problem of scattering of light by a sphere of any size has been solved by Mie.[10] His solution may be discussed in terms of the superposition of the radiation from electric and magnetic dipoles. The center of the spherical particle is taken as the origin of a spherical coordinate system and the Maxwell equations are expressed in this system as second order partial differential equations. The continuity of the radial and angular components of both the electric and magnetic field intensity supplies the necessary boundary conditions. The solutions of these equations are found to be an infinite series of products of associated Legendre polynomials, spherical Bessel functions, and simple trigonometric functions. Each term of the resulting series contains undetermined coefficients. The scattered field and the field due to the incident wave are combined at the surface of the sphere to determine the arbitrary coefficients. The intensity of the scattered light is obtained from the uniquely determined scattered field. The final result of these long and involved calculations can be put in the form

---

[10]Mie, G., Ann. Physik, 25, 377 (1908).

$$J_1 = \frac{\lambda^2}{8\pi^2 r^2} \left| \frac{a_1}{2} + \frac{a_2}{2} \cos\theta + \frac{p_1}{2} \cos\theta + \ldots \right|^2$$

$$J_2 = \frac{\lambda^2}{8\pi^2 r^2} \left| \frac{a_1}{2} \cos\theta + \frac{a_2}{2} \cos 2\theta + p_1 + \ldots \right|^2 \qquad (16)$$

where

J_1 = intensity of the component vibrating perpendicular to the plane of observation;

J_2 = intensity of the horizontal component;

a_1 = electric dipole contribution;

a_2 = electric quadripole contribution;

p_1 = magnetic dipole contribution;

moreover

$$a_1 = 2\alpha^3 \frac{m^2 - 1}{m^2 + 2}$$

$$a_2 = -\frac{\alpha^5}{6} \frac{m^2 - 1}{m^2 + 3/2}$$

$$p_1 = -\frac{\alpha^5}{15} (m^2 - 1)$$

and

$$\alpha = 2\pi R/\lambda .$$

When the radius of the particle is small, only the electric dipole term, a_1, is important and equations (16) reduce to the Rayleigh expression.

For a somewhat larger particle the next two terms which involve a_2 and p_1 must also be considered. These are both

negative and hence will produce an assymmetry in the intensity of the scattered light with more scattered in the forward than backward direction. The horizontally polarized component J_2 is not zero for $\theta = 90^\circ$ and hence the light is no longer completely polarized in this direction.

For very large particles it is necessary to take into account still more terms. The number of these terms which must be included in the sums of equations (16) for practical calculations depends upon the values of α and m. Blumer[11] has calculated angular scattering intensities for isotropic spheres of increasing diameters where m = 1.25. Figure 2 illustrates angular scattering diagrams from those calculations. The large area of forward scattering in B is not

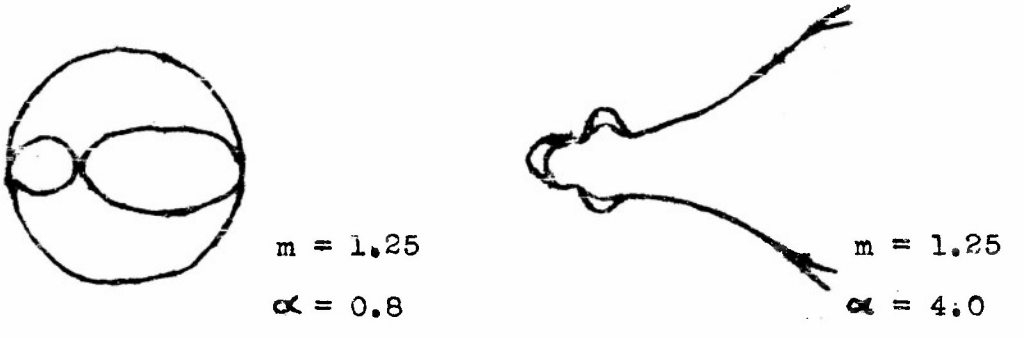

Fig. 2. Radiation Diagram of a Large Sphere

---

[11] Blumer, H., Z. Physik, 32, 119 (1925); 38, 304 (1926); 39, 920 (1926).

completely shown. The complexity of the maxima and minima increase as m and α become larger.

Shoulejkin[12] has carried out the calculations for spherical particles of refractive ratio m = 1.33 and α equal 1, 3, and infinity. More recently the U. S. Bureau of Standards[13] has tabulated numerical values of m = 1.33 to m = 2.00. This range of refractive ratios covers aerosols and suspensions of pigments.

Several light scattering methods based on considerations of the Mie Theory have been developed.

1. Engelhard and Friess,[14] Paranjpe[15] et al., and Ruedy[16] have calculated the Mie terms for large values of α and compared them with measured values determined on aerosols.

2. The depolarization of light scattered at 90° by large isotropic spheres has been used to determine the size of these particles by Pokrowski,[17] van dem Borne,[18] and

---

[12]Shoulejkin, W., Phil. Mag., 48, 307 (1924).

[13]Lowan, A. P., Tables of Scattering Functions for Spherical Particles, Natl. Bureau of Stds., AMS 4 (1949).

[14]Engelhard, H. and Freiss, H., Kolloid Z., 81, 129 (1937).

[15]Paranjpe, G. R., Naik, G. Y. and Vaidya, P. B., Proc. Indian Acad. Sci., A9, 333, 352 (1939).

[16]Ruedy, R., Can. J. Research, A21, 79, 99 (1943); A22, 53 (1944).

[17]Pokrowski, G. I., Z. Physik, 41, 493 (1927); 60, 850 (1930).

[18] van dem Borne, H., Z. Physik, 99, 73 (1936).

Krishnan.[19]

3. If white light is incident upon a scattering particle each color component will exhibit its own scattering diagram and various colors can be seen at different angles. These higher order Tyndall spectra, as they are called, have been investigated by La Mer[20-22] and his coworkers for the case of sulfur sols and they have obtained good agreement with the Mie theory.

4. Another effect observed in the case of large particles is that the scattered intensity at a given angle is no longer proportional to the inverse fourth power of the wave length but to some lesser power. This has led Heller and Vassy[23] to suggest that particle sizes may be ascertained by determining the value of the wave length exponent. Measurements along this line by Heller and his coworkers have shown the method to be a useful one.

5. Pangonis and Heller[24] have arranged the Mie equations

---

[19]Krishnan, R. S., Proc. Indian Acad. Sci., A1, 211 (1934); A2, 221 (1935); A3, 126 (1936).

[20]La Mer, V. K. and Barnes, M. D., J. Coll. Sci., 1, 71 (1946).

[21]La Mer, V. K. and Johnson, I., J. Am. Chem. Soc., 69, 1184 (1947).

[22]La Mer, V. K. and Kenyon, A. S., J. Coll. Sci., 4, 163 (1949).

[23]Heller, W. and Vassy, E., J. Chem. Phys., 14, 565 (1946).

[24]Pangonis, W., Light Scattering by Colloidal Systems, Dissertation, Wayne University (1952).

into practical scattering functions and have compiled calculations covering the range m = 1.05 to m = 1.30 and α = 0.2 to α = 15.0. One of these scattering functions, the specific turbidity, defined as

$$\lim_{c \to 0} \frac{\tau}{c} = \left(\frac{\tau}{c}\right)_0$$

and its variation with particle size is the object of this paper.

CHAPTER III

THE LIGHT SCATTERING APPARATUS

The apparatus used to make the measurements was essentially that designed by W. Heller and K. Herrington.[1] It consists of three main sections: the illuminating unit, the monochromator, and the scattering unit. The schematic diagram (Figure 3) illustrates the main features of the apparatus.

A. The Illuminating Unit

The illuminating unit consists of a lamp housing into which can be inserted either a mercury vapor lamp, type AH-4 or a tungsten ribbon filament lamp, type 18A-10T. The power supply to the lamp is maintained at a constant voltage by means of a Sorensen voltage regulator, Model 500-S. Hence, the intensity of the light source S varies by not more than $\pm$ 1/4 %. The lamps are air-cooled by means of a fan to prevent them from overheating.

The light is first made to pass through a water filled cylinder F with plane parallel windows of optical glass at

---

[1] Herrington, K., A New Method for Determining the Size of Large Mclecules and Polymer Particles, Dissertation, Wayne University (1950).

each end. This serves to filter out the infrared radiation.

The diverging light is then collected and brought to a focus on the monochromator entrance slit M.S. by means of the collimating lenses L_1 and L_2.

B. The Monochromator

Since the light scattering measurements are to be made at a well defined wave length it is necessary to use monochromatic light. The monochromator serves to disperse the light from the source and to permit a selection of the particular wave length desired.

The monochromator entrance slit is preceded by a shutter diaphragm D_1 which can be opened or closed with a cable release, thus controlling the passage of light into the instrument proper. The width of the entrance slit itself can be regulated by means of a graduated knob. The light beam after being rendered parallel by the lens L_3 passes through the monochromator prism P and is brought to a focus on the diaphragm S.E. by means of the lens L_4.

The monochromator prism is a Pellin-Broca constant deviation prism and is mounted on a rotatable platform. A drum calibrated to read directly in wave lengths rotates the prism so that light of the indicated wave length falls on the S.E. diaphragm opening. The monochromator is rigidly mounted with respect to the illuminating unit and the scattering unit.

C. The Scattering Unit

The S.E. diaphragm is a disk with four circular openings of 1, 2, 4 and 10 mm. in diameter. The disk can be rotated so as to bring any of these openings into the optic axis of the instrument.

The beam is rendered parallel by the plano-convex lens L_5 placed at the focal distance from the S.E. diaphragm. This step is exceedingly important since a diverging beam would result in high values for the observed turbidities. If the divergence is defined as the angle measured from the center of the beam to its outer edge then we have in this case a divergence of only 20 minutes. Stray light is removed by the two diaphragms D_3 and D_4.

M is a plane parallel glass plate set at an angle of 45° which reflects about 11% of the light through the side arm PH_1. The reflected beam, which is used as a reference, passes through the three polaroids P_1, P_2, and P_3. Each polaroid can be rotated in six distinct steps through an angle of 90°. By the proper positioning of the polaroids the intensity of the reference beam can be made to approximate that of the light scattered at PH_2 when making measurements of scattering at 90°.

The light in passing through the monochromator prism and the glass plate M becomes partially plane polarized due to selective reflection of the component vibrating parallel to the plane of the glass surfaces. A compensating plate CP

consisting of two glass plates with an air space between them is placed directly in front of the S.E. diaphragm. By adjusting the angle of inclination of the compensator plate the proper amount of the orthogonal component can be removed from the beam. In this manner, the light passing through the glass plate M can be transformed back to natural light.

The main portion of the primary beam passes through the CD diaphragm into the chamber A. The CD diaphragm is any one of five interchangeable metal rings with openings of from one to five mm. in diameter.

For measurements of the turbidity, two 10 cm. cylindrical absorption cells with fused corex windows were used. These were mounted on a special carriage which holds the cells parallel to each other and to the incoming beam of light and which can be fastened into the chamber A. The carriage is designed to allow first one cell then the other to be brought into the optic axis of the instrument. One cell, containing double distilled water is used to obtain the intensity of the reference beam I_o. The other contains the solution whose turbidity is to be determined. It was observed that light scattered through the sides of the latter cell was reflected from the walls of chamber A and picked up by the photocell. Also, secondary scattering in the forward direction by that part of the turbid solution not directly illuminated by the primary beam introduced considerable error. To eliminate these two effects, the sides of the cell were painted

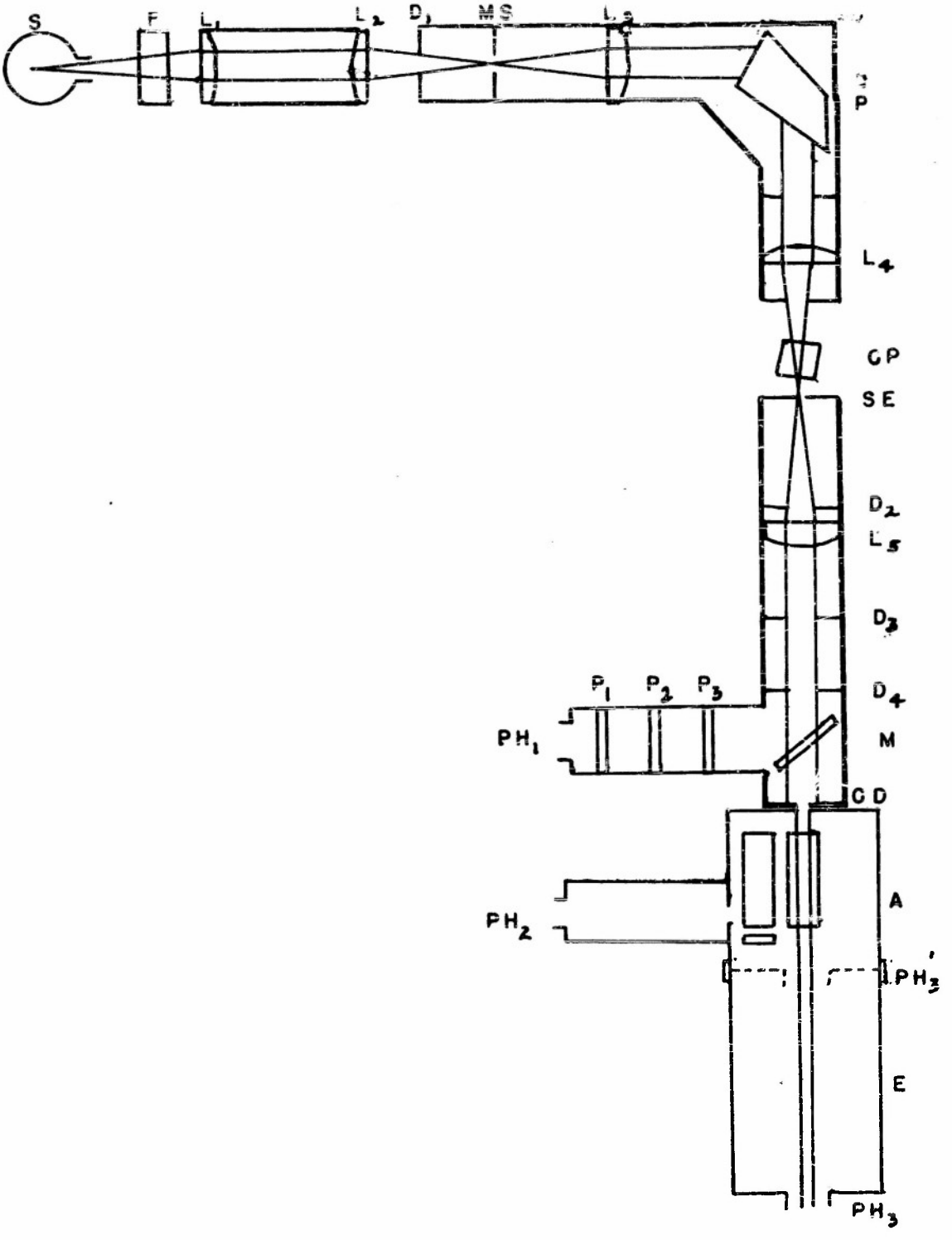

Fig·3 SCHEMATIC DIAGRAM OF LIGHT SCATTERING APPARATUS

black and a diaphragm with an opening slightly larger than the diameter of the beam was placed at the exit end of the cell. Data comparing results obtained before and after blackening the cell are given in Chapter V.

Neutral gray filters of known optical density can be placed in a holder at the exit end of the reference cell. These serve to reduce the difference between the intensity of the reference beam and that of the beam emerging from the turbid solution so that they may be more easily compared.

D. The Solid Angle of Scattering

Since the sensitive area of the photocell necessarily subtends a finite solid angle, not only is the transmitted light measured but also light scattered by the particles within this subtended angle. Obviously, the solid angle varies along the length of the beam but since the most significant contribution to the intensity of the angularly scattered light is made by the particles at the exit end of the transmission cell, we define the solid angle as shown in Fig. 4.

This has the effect of making the measured turbidity appear lower than is actually the case. To reduce the solid angle one or both of two things can be done: the photocell can be further removed from the transmission cell by the addition of the extension E, 25.5 cm. in length, to the end of the scattering unit and/or a 4 mm. diaphragm can be inserted in front of the photocell to decrease its aperture.

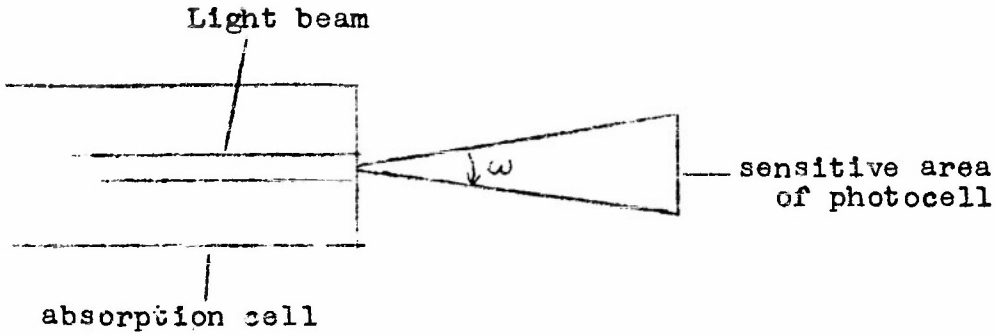

Fig. 4. The Solid Angle of Scattering

Four solid angles can be obtained by the following combinations:

		ω
no extension;	no diaphragm	16.5°
no extension;	diaphragm	10.0°
extension E;	nodiaphragm	2.0°
extension E;	diaphragm	0.8°

The light scattering apparatus as here described has none of the disadvantages of the Beckman spectrophotometer used by some investigators for turbidimetric measurements. One of these is the fact that the primary beam in the latter instrument has a considerable amount of divergence. Even more serious is the fact that since the photocell is located directly behind the absorbtion cell and has a large aperture, a considerable amount of angularly scattered light is also measured (large ω). This latter effect causes the observed turbidities to be much lower then is actually the case.

E. Photoelectric Measuring Device

A multiplier photometer model 520 M, manufactured by the Photovolt Corporation, New York City was used for the measurement of relative light intensities. This is a line operated instrument utilizing an IP 22 photomultiplier tube. It has four sensitivity ranges each differing by a factor of 10 from the succeeding one and a maximum sensitivity of about 10^{-11} lumens per scale division.

CHAPTER IV

EXPERIMENTAL PROCEDURE

A. Preparation of Latex Suspensions

The model systems used in this investigation were fairly monodisperse polystyrene and polyvinyltoluene latices provided by the Dow Chemical Co. These systems were chosen because the particles were known to be spherical thus permitting a direct comparison between the light scattering measurements and the Mie theory. Furthermore, these substances exhibit no absorption in the visible portion of the spectrum.

The mean particle diameter of many of the latices had already been determined upon their receipt by means of the electron microscope. Preparations of the remaining samples suitable for electron microscopy were sent to both Dr. E. B. Bradford of the Dow Chemical Co. and to Dr. John H. L. Watson of the Edsel B. Ford Institute for Medical Research. The size distribution studies of these samples as made in our laboratory from the electron micrographs, as well as those made at Dow, are shown in Table I. The mean particle diameters as determined from the electron micrographs taken at Dow Chemical and from those taken by Dr. Watson differed slightly. This variation is probably due to the different calibration procedure followed by the operators in determining the magnification of the electron microscope. The particle sizes for these samples are accordingly represented in Figure 15

by a line connecting the two values.

The latex samples as received contained 30-50% solids. The preparation of diluted latex for the light scattering measurements was carried out in the following manner: Enough of the latex (two to three cc.) was added to 125 cc. of double distilled water in a centrifuge bottle to reduce the concentration to about 0.5%. The suspension was centrifuged to remove any agglomerates that might have formed in the latex. 100 cc. of the supernatant suspension, hereafter called the master batch, were pipetted into a flask. The concentration of this was determined by accurately weighing out about 25 grams and evaporating to dryness in a partial vacuum at 80° and then weighing the dried solids. A series of dilutions from the master batch were made volumetrically by adding double distilled water to portions measured with a 10 ml. burette into volumetric flasks.

It is noteworthy that all samples were kept in pyrex glassware which had been cleansed with hot detergent and refluxed in steam.

The exclusion of any foreign matter which might contribute noticeably to the scattering is of prime importance. For this reason, double distilled water was used in the preparation of all solutions.

To safeguard against any changes taking place in the suspensions upon prolonged standing, all measurements were made within three days of the time when they were first prepared.

TABLE I. MEAN PARTICLE DIAMETER AND STANDARD DEVIATION OF LATICES

Sample No.	E. B. Bradford			J. H. Watson		
	No. of Particles Counted	Average Diameter m μ	Standard Deviation m μ	No. of Particles Counted	Average Diameter m μ	Standard Deviation m μ
41	84	119	4			
39	74	132	2			
40	76	144	4			
42	79	177	4			
2023*	352	230	9	334	218	8
2022*	202	254	10	259	258	9
7065*	187	252	35	270	263	36
7194*	234	275	47	305	299	57
2012	-	-	-	269	373	11
43B	-	439	6			
44A	29	470	5			
43C	-	535	9			
44B	20	595	7			
44C	21	770	11			

*Starred data refer to polystyrene, others pertain to polyvinyltoluene

B. Calibration of Gray Filters

For those latex suspensions whose transmissions were an order of magnitude less than that of the reference cell it was found convenient to employ neutral gray filters to reduce the intensity of the light transmitted by the reference cell. By thus making the two beams comparable, their intensity could be read on the same sensitivity setting of the photometer. Hence, by not changing the sensitivity of the instrument from one reading to the next, any error introduced by a deviation from a strictly 10:1 ratio of the sensitivity could be avoided.

Two gray filters having an optical density of approximately 1 and 2 respectively were used in measuring the turbidity. These were calibrated in the light scattering apparatus at a wave length of 546.1 mμ (Table II).

TABLE II. TRANSMISSION OF GRAY FILTERS

	I_0/I
GF-1 #2	11.3
GF-2	112

However, it was later shown that the sensitivity settings of the photometer conformed strictly to a 10:1 ratio thereby making optional the use of the gray filters.

C. Measurement of the Turbidity

A mercury arc lamp was used as a light source and all measurements of the turbidity were made with the green line (λ = 546.1 mμ). The monochromator entrance slit was set

at a reading of 22. The S.E. diaphragm was set at the 1 mm, opening and a CD diaphragm of 2 mm. was employed.

The turbidity, τ , is defined by equation (3) as:

$$\tau = \frac{\ln I_o/I}{l}$$

Experimentally, τ was determined by filling one absorption cell with the latex suspension and the other with double distilled water. Consecutive measurements of the intensity of the light passing through the distilled water cell (reference cell), I_o, and that passing through the latex, I, permit a direct calculation of τ .

Although supposedly matched, the transmission of the two absorption cells when filled with water was not always the same. This was probably due to an adsorbed polymer film on the faces of the cell. Therefore, it sometimes became necessary to correct the observed turbidities of the latex suspensions by the apparent turbidity of the absorption cell. This correction term was determined after running each series of measurements since its value changed from time to time.

CHAPTER V

EXPERIMENTAL RESULTS

A. The Specific Turbidity Using the Unblackened Cell

Tables III-XVI summarize the experimental results obtained with the use of the unblackened transmission cell. All of these data, as well as those discussed in Part B, were taken under conditions giving a solid angle of 2.0°. Figures 5 and 6 show the variation of turbidity with concentration. At low concentrations these are all straight lines with the slope increasing as the particle size increases. For the larger particles at higher concentrations, the turbidity ceases to be a linear function of concentration. Furthermore, the larger the particle size the lower is the concentration at which the deviation from linearity begins. This is a result of secondary scattering into the photocell from those parts of the solution not directly illuminated by the primary beam as well as some reflected light from the inner walls of the chamber containing the trasmission cell, these effects becoming more prominent the higher the turbidity.

The plot of the specific turbidity, τ/c, as a function of concentration, Figures 7-9, is a straight line readily extrapolated to infinite dilution for particles with diameters less than 300 mμ. For larger particles, however, the lines curve down sharply. This, as already mentioned, is due to reflected and secondary scattered light.

B. The Specific Turbidity Using the Blackened Cell

Tables XVII-XXX give the experimental results obtained using the blackened cell. Figures 10 and 11 again show the variation of turbidity with concentration but now all lines are very nearly straight within the concentration range studied. This is due to the fact that the amount of reflected and secondary scattered light has been reduced to a minimum.

In Figures 12-14 the specific turbidity is plotted against concentration and extrapolated to infinite dilution but, in contrast to Figures 7-9, these lines are all nearly horizontal. It should be noted, however, that the extrapolated value, $(\tau/c)_o$, for a given sample is not significantly different in the two cases and, except for sample 44B, any differences that do exist are within experimental error. Nevertheless, use of the blackened cell is preferred since the extrapolation to infinite dilution is much more secure particularly when dealing with particles whose diameters are in excess of 300 mμ.

The variation of $(\tau/c)_o$ with particle size is shown in Figure 15. The mean particle diameters as determined by the two different electron microscopists are accordingly designated by a horizontal line connecting the two values.

A comparison of the experimentally determined $(\tau/c)_o$ values with those calculated by Heller and Pangonis[1] from the Mie theory is made in Table XXXI.

---

1. W. Heller and W. J. Pangonis; J. Chem. Phys., 22, 948 (1954).

TABLE XXXI

$(\tau/c)_o$ cm^{-1}	D_o mμ	D_e mμ		% deviation
		Bradford	Watson	
5.1*	58	45	65	-28.9 (Epel)
22.9	109	119	-	8.4
37.0	132	132	-	0
49.4*	132	135	155	2.2 (Epel)
42.7	141	144	-	2.1
59.0*	152	150	180	- 1.3 (Epel)
62.7	171	177	-	3.4
104.2*	206	219	258	5.9 (Epel)
110.9*	215	223	260	3.6 (Epel)
109.4*	212	230	218	7.8
113.0*	217	254	258	14.5
126.0*	232	252	263	7.9
126.0*	232	259	289	10.4 (Epel)
158.4*	262	275	299	4.7
204	350	-	373	6.2
246	410	439	-	6.6
269	446	470	-	5.1
310	511	535	-	4.5
331	548	595	-	7.9
397	705	770	-	8.4

*Starred data refer to polystyrene, others pertain to polyvinyltoluene.

The first column gives the experimental specific turbidities extrapolated to zero concentration. The second column contains the optical particle diameters, D_o, calculated by interpolation from the theoretical specific turbidities. This required an accurate knowledge of the refractive index and density of the polymeric substances. A separate study in this laboratory by T. L. Pugh[2] showed that the colloidal spheres of polystyrene and polyvinyl toluene had a density of 1.057 and 1.026 and a refractive index of 1.625 and 1.595 respectively at 25.0° C. Columns 3 and 4 show the electron microscopic diameters, D_e, and Column 5 gives the per cent deviation of electron optical diameters (Bradford) from the optical ones. Excluding from a comparison the unsatisfactory sample with the smallest particle size, the average per cent deviation is 5.6. If the diameters obtained by Watson are used the average deviation becomes 14.5. Specific turbidities obtained earlier by J. N. Epel[3] are also included in Table XXXI.

The refractive indices reported above represent values extrapolated to zero particle size. There is evidence that this may not be entirely warranted and that a truer value is

---

2. T. L. Pugh, The Refractive Index and Density of Polystyrene and Polyvinyl Toluene Latices, O.N.R. Project NR 330-027, Tech. Report 7.

3. J. N. Epel; Light Scattering Methods for Determining the Size of Large Colloidal Particles, Dissertation, Wayne University (1951).

obtained by taking the average refractive index over a particle size range of 0-400 mμ. If this is done the refractive indices for polystyrene and polyvinyl toluene become 1.607 and 1.588 respectively. Use of these values to determine D_0 reduces the average per cent deviation to 3.4 (Bradford).

The systematic error in electron microscopy should not exceed, but may be as large as 5% and the non-systematic error is assumed to be about 1%. The error in measurements of $(\tau/c)_0$ is approximately 3%. Taking all this into account, the agreement between optical and electron optical diameters must be considered as excellent.

C. Variation of Specific Turbidity with Solid Angle

The solid angle of the secondary beam subtended by the photocathode is a potential source of error in turbidity measurements (Chapter III). Data exemplifying this effect are given in Table XXXII and Figures 16-20 where τ/c is plotted against concentration. The rapid decline exhibited in Figures 17, 19, and 20 can be attributed to the increased amount of light scattered in the forward direction by large particles and hence included within the solid angle.

The dependence of τ/c on the solid angle at different concentrations is more clearly brought out in Figures 21 and 22. The most significant line in these figures is the zero concentration line since it is the specific turbidity at infinite dilution, $(\tau/c)_0$, which is to be related to particle size. For small particles (D = 177 mμ). This line

is horizontal and, in general, increases in slope as the particle size increases. However, the maximum deviation of $(\tau/c)_o$ within the range studied is never greater than 1.3% of the extrapolated value at zero solid angle.

For the most precise work, then, it is desirable to have as low a solid angle as practical considerations will permit since the error in $(\tau/c)_o$ is not only lessened but the τ/c vs. c line is straight over a wider concentration range thereby facilitating extrapolation to zero concentration.

D. Specific Turbidities Using the Beckman Spectrophotometer.

Use of the Beckman spectrophotometer for the purpose of determining turbidities has been reported by some investigators. In order to ascertain the usefulness of the instrument for this purpose, comparative studies were undertaken using a Beckman spectrophotometer, model DU. The results obtained using a 1 cm. cell at a wave length of 5461 A and a slit width of 0.045 mm. are tabulated in Table XXXIII and shown graphically in Figure 23.

It is immediately apparent that the $(\tau/c)_o$ values are considerably lower than those obtained with the light scattering apparatus. The variation of the % difference between the two sets of values with particle size is given by curve A of Figure 24.

In order to get a more direct comparison, a 10 cm. cell attachment was added to the spectrophotometer and a blackened 10 cm. absorption cell was used with a diaphragm slightly

larger than the beam of light at the exit end. The slit width was set at 0.08 mm. Table XXXIV and Figure 20 show the results obtained. The % difference between these $(\tau/c)_o$ values and those from the light scattering apparatus are given in Curve B of Figure 24.

The considerably lower values of $(\tau/c)_o$ as determined with the Beckman instrument, whether using the 1 cm. or blackened 10 cm. cell, can be attributed to the rather large solid angle of scattering, about 35^o, resulting from the proximal position of the photocell to the absorption cell. The slit width and the diameter of the beam may also play some part in determining the error although these factors have not been investigated. In any event, it is obvious that the Beckman spectrophotometer as such is not of any value for the direct determination of particle sizes from specific turbidity.

TABLE III. SPECIFIC TURBIDITY

Sample 41 D = 119 mμ

c^* x 10^3	I_o/I x 10^{-1}	τ	τ/c
0			(21.1)**
1.152	0.128_2	.0247	21.4
2.304	0.167_3	.0513	22.3
3.456	0.215_3	.0765	22.1
4.608	0.285_6	.1050	22.78
5.760	0.378_8	.1332	23.12
6.912	0.506_8	.1623	23.48

TABLE IV. SPECIFIC TURBIDITY

Sample 39 D = 132 mμ

c^* x 10^3	I_o/I x 10^{-1}	τ	τ/c
0			(35.0)**
1.273	0.160_2	.0470	36.9
2.546	0.243_0	.0888	34.8
3.819	0.381_2	.1338	35.04
5.092	0.595_9	.1785	35.05
6.365	0.922_6	.2222	34.91
7.638	1.45_2	.2674	35.00
10.18	3.52_4	.3561	34.98
12.73	8.34_7	.4425	34.76

TABLE V. SPECIFIC TURBIDITY

Sample 40 D = 144 mμ

c^* x 10^3	I_o/I x 10^{-1}	τ	τ/c
0			(42.7)**
1.182	0.164_6	.0501	42.4
2.364	0.273_4	.1004	42.47
3.546	0.440_8	.1484	41.85
4.728	0.734_5	.1994	42.17
5.910	1.20_0	.2485	42.05
7.092	1.97_1	.2980	42.02
9.456	5.33_5	.3978	42.07
11.82	14.0_1	.4942	41.81

*Concentration expressed as grams of solids per 100 grams of latex.

**Extrapolated value.

TABLE VI. SPECIFIC TURBIDITY

Sample 42 D = 177 mμ

c^* x 10^3	I_o/I x 10^{-1}	τ	τ/c
0			(63.1)**
0.5610	0.140_3	.0336	59.9
1.122	0.202_2	.0703	62.7
1.683	0.287_5	.1058	62.86
2.244	0.405_6	.1401	62.43
3.366	0.800_0	.2079	61.76
4.488	1.59_0	.2766	61.63
5.610	3.11_0	.3437	61.27

TABLE VII. SPECIFIC TURBIDITY

Sample 2023 D = 218-230 mμ

c^* x 10^3	I_o/I x 10^{-1}	τ	τ/c
0			(108)**
0.6742	0.207_2	.0728	108
1.011	0.296_4	.1085	107.3
1.348	0.429_4	.1456	108.0
2.023	0.894_1	.2191	108.3
2.697	1.83_3	.2907	107.8
3.371	3.77_0	.3630	107.7
4.045	7.86_4	.4364	107.9
5.394	32.3_8	.5781	107.2

TABLE VIII. SPECIFIC TURBIDITY

Sample 2022 D = 254-258 mμ

c^* x 10^3	I_o/I x 10^{-1}	τ	τ/c
0			(111.3)**
0.6767	0.211_9	.0751	111
1.015	0.310_9	.1135	111.8
1.353	0.448_4	.1500	110.9
2.030	0.952_2	.2253	111.0
2.707	2.03_8	.3015	111.4
3.384	4.28_7	.3759	111.1
4.060	8.95_7	.4495	110.7
5.414	39.5_3	.5979	110.4

*Concentration expressed as grams of solids per 100 grams of latex.

**Extrapolated value.

TABLE IX. SPECIFIC TURBIDITY

Sample 7065 D = 252-263 mμ

c* x 10^3	$I_o/I \times 10^{-1}$	τ	τ/c
0			(126)**
0.5295	0.192_3	.0652	123
1.059	0.375_7	.1324	125.0
1.588	0.722_5	.1978	124.6
2.118	1.37_6	.2624	123.9
3.177	5.14_3	.3940	124.0
4.236	18.2_3	.5204	122.9
5.295	64.8_6	.6475	122.3

TABLE X. SPECIFIC TURBIDITY

Sample 7194 D = 275-299 mμ

c* x 10^3	$I_o/I \times 10^{-1}$	τ	τ/c
0			(158)**
0.7719	0.316_8	.1154	149.5
1.158	0.601_4	.1793	154.8
1.544	1.08_6	.2388	154.7
2.316	3.27_2	.3487	150.6
3.088	10.5_8	.4663	151.0
3.860	31.3_7	.5749	148.9
4.631	92.8_2	.6833	147.5

TABLE XI. SPECIFIC TURBIDITY

Sample 2012 D = 373 mμ

c* x 10^3	$I_o/I \times 10^{-1}$	τ	τ/c
0			(203)**
0.6242	0.353_6	.1264	202.5
0.9363	0.662_7	.1892	202.1
1.248	1.24_0	.2517	201.7
1.561	2.28_2	.3127	200.3
1.873	4.25_0	.3750	200.2
2.497	14.0_3	.4942	197.9
3.121	44.1_6	.6091	195.2

*Concentration expressed as grams of solids per 100 grams of latex.

**Extrapolated value.

TABLE XII. SPECIFIC TURBIDITY

Sample 43 B — D = 439 mμ

c^* x 10^3	I_o/I x 10^{-1}	τ	τ/c
0			(234)**
0.4415	0.285_8	.1047	237.1
0.8830	0.777_5	.2052	232.4
1.325	2.18_4	.3082	232.6
1.766	6.02_3	.4098	232.0
2.208	15.4_8	.5043	228.4
2.649	39.7_6	.5986	226.0
3.532	150.9	.7321	207.3

TABLE XIII. SPECIFIC TURBIDITY

Sample 44 A — D = 470 mμ

c^* x 10^3	I_o/I x 10^{-1}	τ	τ/c
0			(267)**
0.5727	0.460_0	.1526	266.5
1.145	2.08_3	.3035	265.1
1.718	9.30_4	.4533	263.9
2.291	37.1_3	.5916	258.2
2.864	116.3	.7058	246.4
3.436	254.0	.4841	228.2
4.582	534.8	.8587	187.4

TABLE XIV. SPECIFIC TURBIDITY

Sample 43 C — D = 535 mμ

c^* x 10^3	I_o/I x 10^{-1}	τ	τ/c
0			(297)**
0.4370	0.364_4	.1292	295.7
0.8740	1.33_2	.2587	296.0
1.311	5.00_0	.3912	298.4
1.748	17.2_0	.5147	294.5
2.622	116.2	.7058	269.2
3.496	289.5	.7974	228.1
4.370	432.8	.8375	191.6

*Concentration expressed as grams of solids per 100 grams of latex.

**Extrapolated value.

TABLE XV. SPECIFIC TURBIDITY

Sample 44 B — D = 595 mμ

$c^* \times 10^3$	$I_o/I \times 10^{-1}$	τ	τ/c
0			(310)**
0.8273	1.29_7	.2565	310.0
1.655	16.2_9	.5094	307.8
2.482	95.2_9	.6860	276.4
3.309	199.2	.7597	229.6
4.137	258.8	.7861	190.0
4.964	348.8	.8159	164.4
6.618	533.3	.8583	129.7

TABLE XVI. SPECIFIC TURBIDITY

Sample 44 C — D = 770 mμ

$c^* \times 10^3$	$I_o/I \times 10^{-1}$	τ	τ/c
0			(410)**
0.4191	0.548_1	.1701	405.9
0.8382	2.67_0	.3285	391.0
1.257	12.4_8	.4828	384.1
1.676	44.6_1	.6100	364.0
2.515	157.7	.7367	292.9
3.353	248.0	.7816	233.2
4.191	333.1	.8112	193.6

*Concentration expressed as grams of solids per 100 grams of latex.

**Extrapolated value.

TABLE XVII. SPECIFIC TURBIDITY

Sample 41 D = 119 mμ

$c^* \times 10^3$	$I_o/I \times 10^{-1}$	τ	τ/c
0			(22.9)**
1.039	$.126_6$	.02355	22.67
2.078	$.162_8$	.05074	23.48
3.117	$.203_9$	.07125	22.86
4.156	$.260_9$	.09587	23.07
5.195	$.347_7$	.1246	23.98
6.234	$.437_4$	.1475	23.66
8.312	$.727_3$	.1984	23.87
10.39	1.15_7	.2448	23.56

TABLE XVIII. SPECIFIC TURBIDITY

Sample 39 D = 132 mμ

$c^* \times 10^3$	$I_o/I \times 10^{-1}$	τ	τ/c
0			(37.0)**
1.055	$.148_1$	.03927	37.22
2.110	$.216_0$	.07701	36.50
3.165	$.329_2$	.1191	37.63
4.220	$.466_7$	.1540	36.49
5.275	$.716_7$	.1969	37.33
6.330	1.02_1	.2323	36.70
8.440	2.32_3	.3145	37.26
10.55	4.75_8	.3862	36.61

TABLE XIX. SPECIFIC TURBIDITY

Sample 40 D = 144 mμ

$c^* \times 10^3$	$I_o/I \times 10^{-1}$	τ	τ/c
0			(42.7)**
1.014	$.153_8$	.04301	42.42
2.028	$.235_0$	.08544	42.18
3.042	$.369_0$	.1306	42.93
4.056	$.578_5$	.1755	43.27
6.084	1.33_8	.2593	42.62
8.112	3.26_3	.3485	42.96
10.14	7.30_8	.4291	42.32

*Concentration expressed as grams of solids per 100 grams of latex.

**Extrapolated value.

TABLE XX. SPECIFIC TURBIDITY

Sample 42 D = 177 mμ

c^* x 10^3	I_o/I x 10^{-1}	τ	τ/c
0			(62.7)**
0.9536	$.181_2$	.05944	62.33
1.907	$.329_4$	.1192	62.51
2.861	$.600_0$	.1792	62.64
3.814	1.10_0	.2398	62.87
4.768	1.96_4	.2977	62.44
5.722	3.54_7	.3569	62.37
7.629	11.4_1	.4737	62.09
9.536	37.7_5	.5934	62.23

TABLE XXI. SPECIFIC TURBIDITY

Sample 2023 D = 218-230 mμ

c^* x 10^3	I_o/I x 10^{-1}	τ	τ/c
0			(109.4)**
0.6317	$.199_5$	.06906	109.3
1.263	$.392_4$	.1367	108.2
1.895	$.801_7$	.2081	109.8
2.527	1.58_0	.2760	109.2
3.159	3.18_5	.3461	109.6
3.790	6.06_4	.4105	108.3
5.054	24.5_1	.5501	108.8
6.317	95.7_8	.6865	108.7

TABLE XXII. SPECIFIC TURBIDITY

Sample 2022 D = 254-258 mμ

c^* x 10^3	I_o/I x 10^{-1}	τ	τ/c
0			(113)**
1.280	$.389_5$	.1424	111.3
1.921	$.884_2$	.2179	113.4
2.561	1.78_5	.2881	112.5
3.841	7.54_7	.4323	112.5
5.122	32.1_4	.5772	112.7
6.402	135.5	.7212	112.7

*Concentration expressed as grams of solids per 100 grams of latex.

**Extrapolated value.

TABLE XXIII. SPECIFIC TURBIDITY

Sample 7065 D = 252-263 mμ

$c^* \times 10^3$	$I_o/I \times 10^{-1}$	τ	τ/c
0			(126)**
0.9275	$.321_6$	.1168	125.9
1.855	1.03_7	.2338	126.0
2.783	3.40_1	.3527	126.7
3.710	10.5_8	.4661	125.6
4.638	34.1_6	.5834	125.8
5.565	107.9	.6984	125.5
7.420	1041.	.9252	124.7

TABLE XXIV. SPECIFIC TURBIDITY

Sample 7194 D = 275-299 mμ

$c^* \times 10^3$	$I_o/I \times 10^{-1}$	τ	τ/c
0			(158.4)**
0.8886	$.401_3$	.1389	156.3
1.777	1.65_9	.2809	158.1
2.666	6.74_3	.4211	158.0
3.554	27.1_0	.5602	157.6
4.443	110.3	.7006	157.7
5.332	443.8	.8390	157.4

TABLE XXV. SPECIFIC TURBIDITY

Sample 2012 D = 373 mμ

$c^* \times 10^3$	$I_o/I \times 10^{-1}$	τ	τ/c
0			(203.6)**
0.6708	$.390_8$	.1363	203.2
1.342	1.51_4	.2717	202.5
2.012	5.83_5	.4066	202.1
2.683	22.4_7	.5415	201.8
4.025	314.1	.8054	200.1
5.366	4458.	1.071	199.6

*Concentration expressed as grams of solids per 100 grams of latex.

**Extrapolated value.

TABLE XXVI. SPECIFIC TURBIDITY

Sample 43B D = 439 mμ

$c^* \times 10^3$	$I_o/I \times 10^{-1}$	τ	τ/c
0			(246)**
0.2866	$.200_6$	.06959	242.8
0.5732	$.413_2$	.1418	247.3
1.146	1.68_7	.2825	246.5
1.433	3.33_6	.3507	244.7
1.720	6.97_9	.4245	246.8
2.293	27.8_9	.5631	245.6
2.866	$107._7$	.6981	243.6
5.732(1 cm cell)	4.10_5	1.413	246.5

TABLE XXVII. SPECIFIC TURBIDITY

Sample 44A D = 470 mμ

$c^* \times 10^3$	$I_o/I \times 10^{-1}$	τ	τ/c
0			(269)**
0.4701	$.352_7$	.1260	268.0
0.9402	1.24_3	.2519	267.9
1.410	4.45_5	.3797	269.3
1.880	15.7_4	.5059	269.1
2.821	192.6	.7565	268.2
3.761	2304.	1.005	267.2

TABLE XXVIII. SPECIFIC TURBIDITY

Sample 43C D = 535 mμ

$c^* \times 10^3$	$I_o/I \times 10^{-1}$	τ	τ/c
0			(310)**
0.3000	$.247_4$	.09058	301.9
0.6000	$.641_7$	.1860	310.0
0.9000	1.59_9	.2771	307.9
1.200	4.12_1	.3718	309.8
1.500	10.0_3	.4607	307.1
1.800	24.3_0	.5492	305.1
2.400	$154._7$	.7345	306.0
3.000	$916._2$	.9124	304.1

---

*Concentration expressed as grams of solids per 100 grams of latex.

**Extrapolated value.

TABLE XXIX. SPECIFIC TURBIDITY

Sample 44B — D = 595 mμ

$c^* \times 10^3$	$I_o/I \times 10^{-1}$	τ	τ/c
0			(331)**
0.4337	$.420_0$	.1435	330.9
0.8674	1.82_6	.2904	334.8
1.301	7.27_4	.4287	329.5
1.735	30.7_4	.5728	330.1
2.169	$128._0$	.7156	329.9
2.602	$519._1$	.8556	328.8
3.470	7409.	1.121	323.1

TABLE XXX. SPECIFIC TURBIDITY

Sample 446 — D = 770 mμ

$c^* \times 10^3$	$I_o/I \times 10^{-1}$	τ	τ/c
0			(397)**
0.3420	0.387_8	.1355	396.2
0.6840	1.51_2	.2716	397.1
1.026	6.14_7	.4118	401.4
1.368	22.6_9	.5424	396.5
1.710	87.6_3	.6775	396.2
2.052	$338._7$	.8129	396.2

*Concentration expressed as grams of solids per 100 grams of latex.

**Extrapolated value.

TABLE XXXII. VARIATION OF SPECIFIC TURBIDITY WITH SOLID ANGLE

Sample 42 D = 177 mμ

$c \times 10^3 \backslash \omega$	0.8°	2.0°	10.0°	16.5°
0		(62.7)*	(62.7)	(62.8)
.9536		62.33	62.79	62.63
1.907		62.51	-	62.56
2.861		62.64	62.39	62.22
4.768		62.44	62.12	62.00
5.722		62.37	62.51	62.11
7.629	61.97	62.09	61.96	61.70
9.536		62.23	61.87	61.48

Sample 7065 D = 252-263 mμ

0		(126.0)	(125.1)	(124.6)
.9275		125.9	-	122.0
1.855		126.0	125.6	124.6
2.783		126.7	124.3	123.6
3.710		125.6	124.8	124.7
4.638		125.8	124.7	124.0
5.565		125.5	124.8	124.5
7.420	124.5	124.7	124.6	123.8

Sample 44A D = 470 mμ

0	(272.0)	(272.0)	(269.2)	(267.5)
.6134	273.2	273.5	267.9	265.0
1.227	272.4	271.9	269.7	268.1
1.840	269.6	270.0	267.9	266.8
2.454	270.7	271.4	269.3	266.6
3.067	272.9	272.4	268.7	264.6
3.680	271.1	272.0	265.7	260.5

* Parenthesis represent extrapolated values.

TABLE XXXII. VARIATION OF SPECIFIC TURBIDITY WITH SOLID ANGLE

Sample 44B D = 595 mμ

$c \times 10^3$ \ ω	0.8°	2.0°	10.0°	16.5°
0	(326.5)	(326.5)	(323.5)	(321.5)
.3685	318.6	318.3	319.7	319.9
.7370	324.7	325.1	324.4	321.4
1.105	326.4	326.1	323.0	321.0
1.474	326.6	327.7	324.8	320.2
1.842	325.4	325.6	320.2	317.2
2.211	325.2	325.1	318.5	315.1
2.948	321.8	320.9	312.4	304.4
3.685	-	311.3	294.2	280.6

Sample 44C D = 770 mμ

0	(404)	(403)	(401)
.3814	403.8	395.1	394.3
.7628	403.0	400.6	397.5
1.144	400.5	396.8	392.7
1.526	402.4	395.2	389.2
1.907	399.9	390.0	381.2
2.288	398.4	382.0	370.1
3.051	383.2	343.5	330.7

TABLE XXXIII. SPECIFIC TURBIDITIES USING THE BECKMAN SPECTROPHOTOMETER

Sample 40 D = 144 mμ

c x 10^3		τ/c
0		(38.5)
1.858	.07324	39.42
3.716	.1415	38.08
5.573	.2111	37.88
7.431	.2927	39.39
9.289	.3570	38.43
27.87	1.056	37.89

Sample 7065 D = 252-263 mμ

0		(110)
.9716	.1053	108.4
1.943	.2143	110.3
2.915	.3286	112.7
3.886	.4305	110.8
5.830	.6445	110.5
7.773	.8557	110.1
9.716	1.027	105.7
19.43	1.897	97.6
29.15	2.551	87.5

Sample 2012 D = 373 mμ

0		(170)
.4819	.07603	157.8
.9638	.1621	168.2
1.928	.3148	163.3
2.891	.4511	156.0
3.855	.6016	156.1
4.819	.7338	152.3
9.638	1.347	139.8
14.46	1.884	130.3

TABLE XXXIII. SPECIFIC TURBIDITIES USING THE BECKMAN SPECTROPHOTOMETER

Sample 44A D = 470 mμ

$c \times 10^3$		τ/c
0		(200)
.5080	.1016	200.0
1.016	.2094	206.1
2.032	.4021	197.9
3.048	.5906	193.8
4.064	.7613	187.3
5.080	.9215	181.4
7.620	1.302	170.8
10.16	1.650	162.4
15.24	2.189	143.6

Sample 44B D = 595 mμ

0		(201)
.4215	.07973	189.2
.8430	.1723	204.4
1.265	.2523	199.4
1.686	.3271	194.0
2.108	.3988	189.2
2.529	.4681	185.1
3.372	.6163	182.8
4.215	.7381	175.1
8.430	1.343	159.3
12.65	1.826	144.3

TABLE XXXIV. SPECIFIC TURBIDITIES USING THE BECKMAN SPECTROPHOTOMETER WITH BLACKENED ABSORPTION CELL

Sample 43C D = 535 mμ

c x 10^3		τ/c
0		(247)
.2753	.06731	244.5
.5506	.1321	239.9
.8259	.1930	233.7
1.101	.2444	222.0
1.652	.3247	196.5
2.202	.3995	181.4

Sample 44C D = 770 mμ

0		(293)
.1744	.04988	286.0
.3488	.09795	280.8
.5232	.1415	270.5
.6976	.1819	260.8
1.046	.2568	245.5
1.395	.3131	224.4

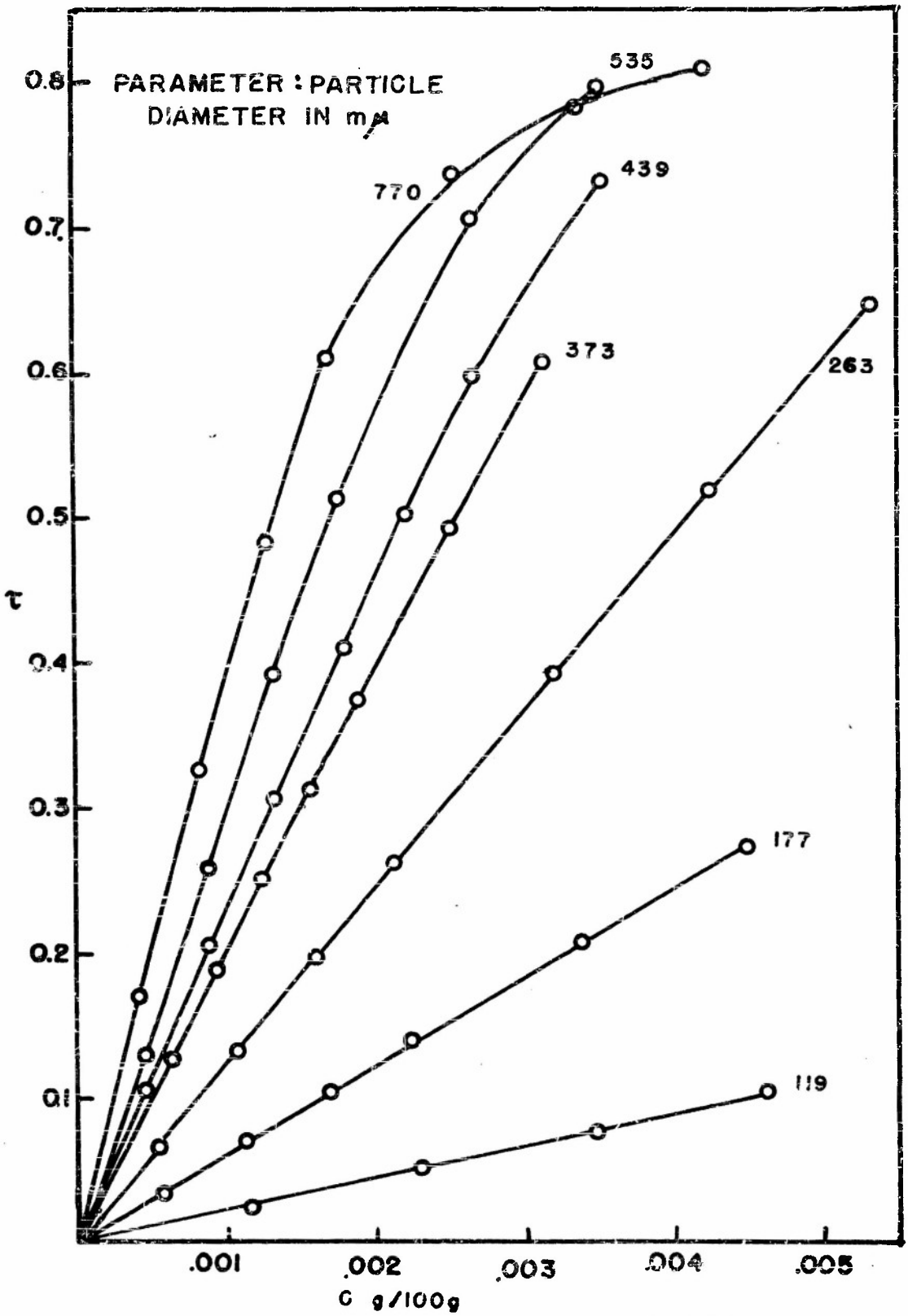

Fig. 5 TURBIDITY AS A FUNCTION OF CONC.

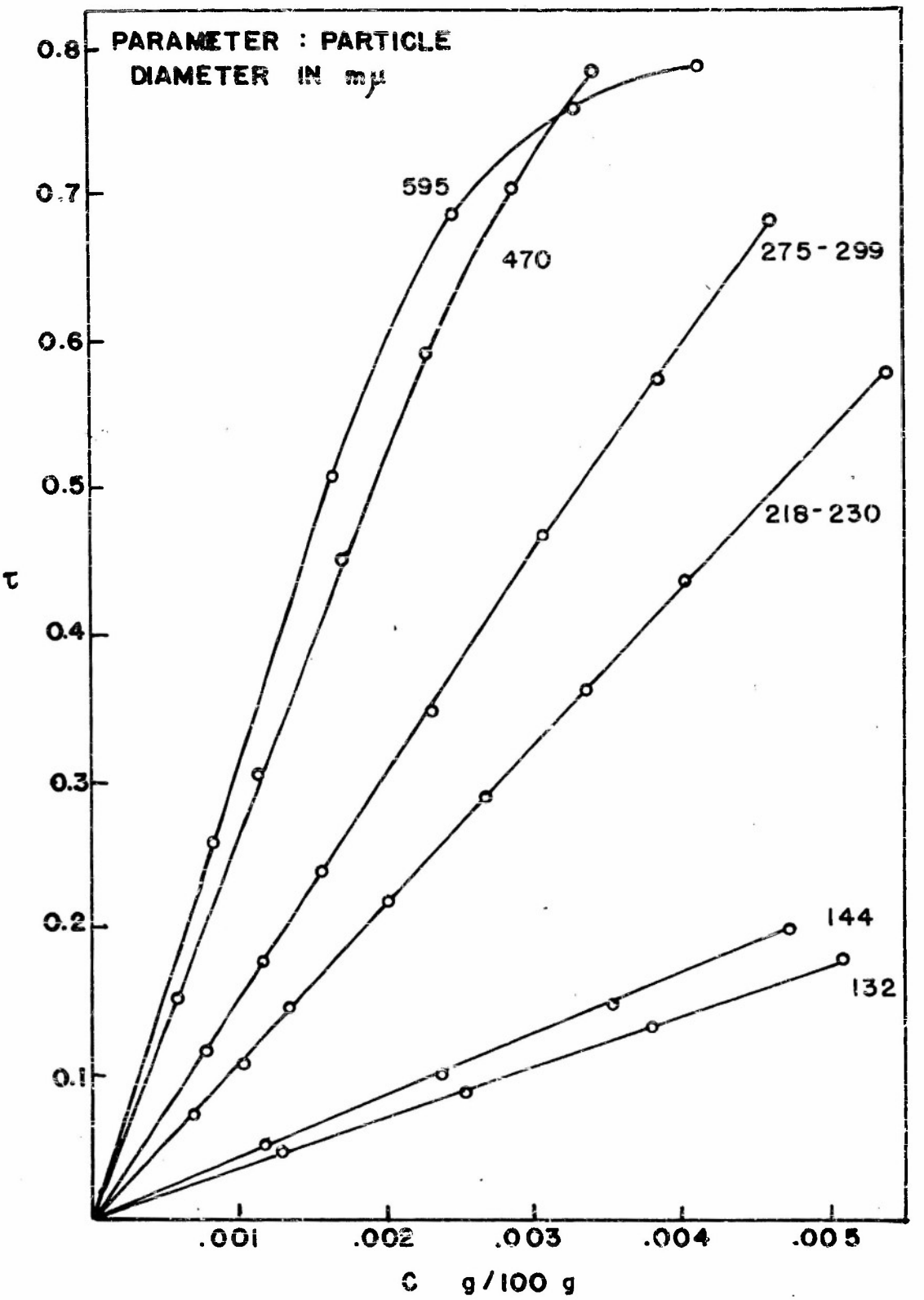

FIG. 6 TURBIDITY AS A FUNCTION OF CONC.

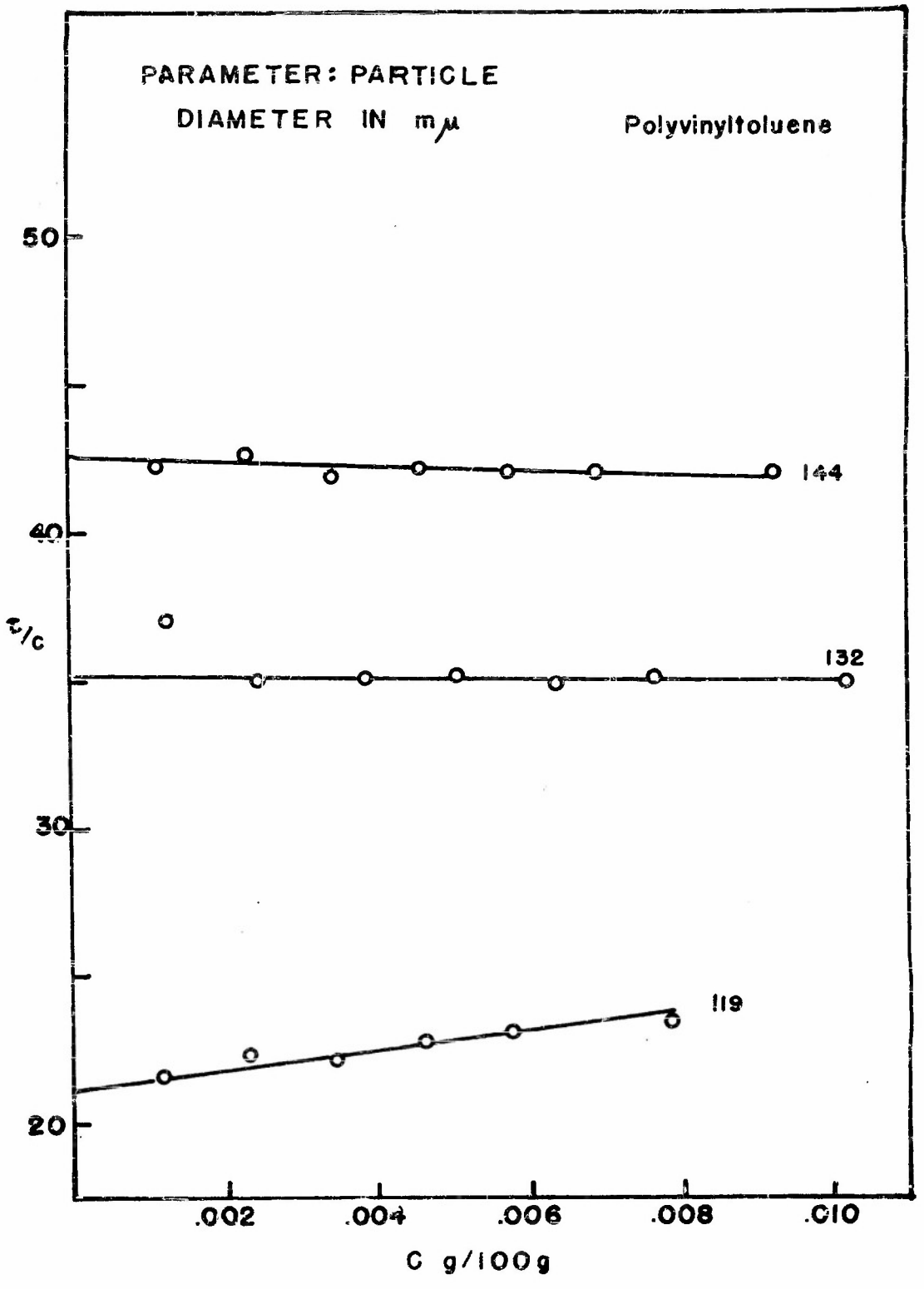

Fig. 7 SPECIFIC TURBIDITY vs. CONC.

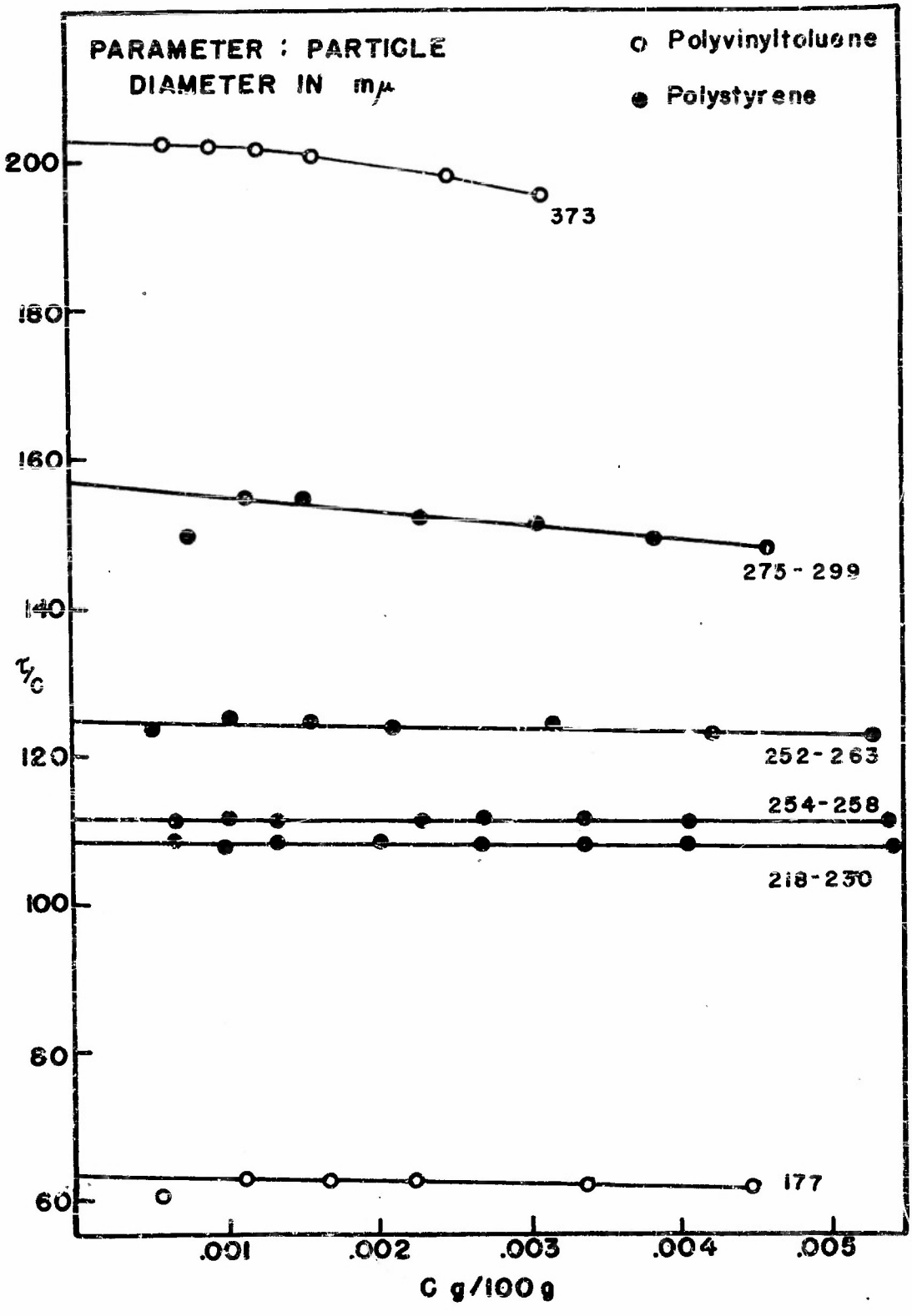

Fig. 8 SPECIFIC TURBIDITY vs. CONC.

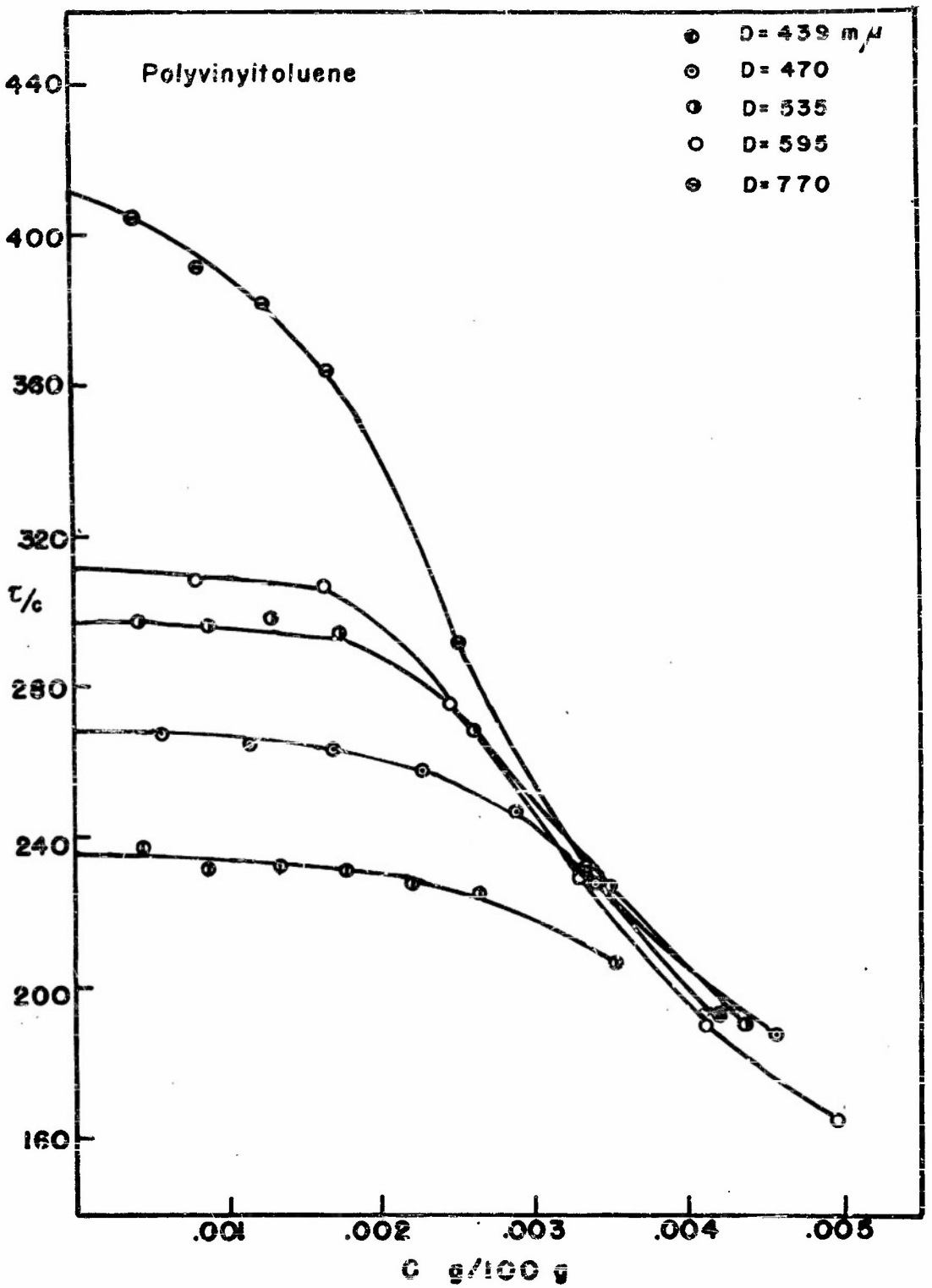

Fig. 9 SPECIFIC TURBIDITY vs. CONC.

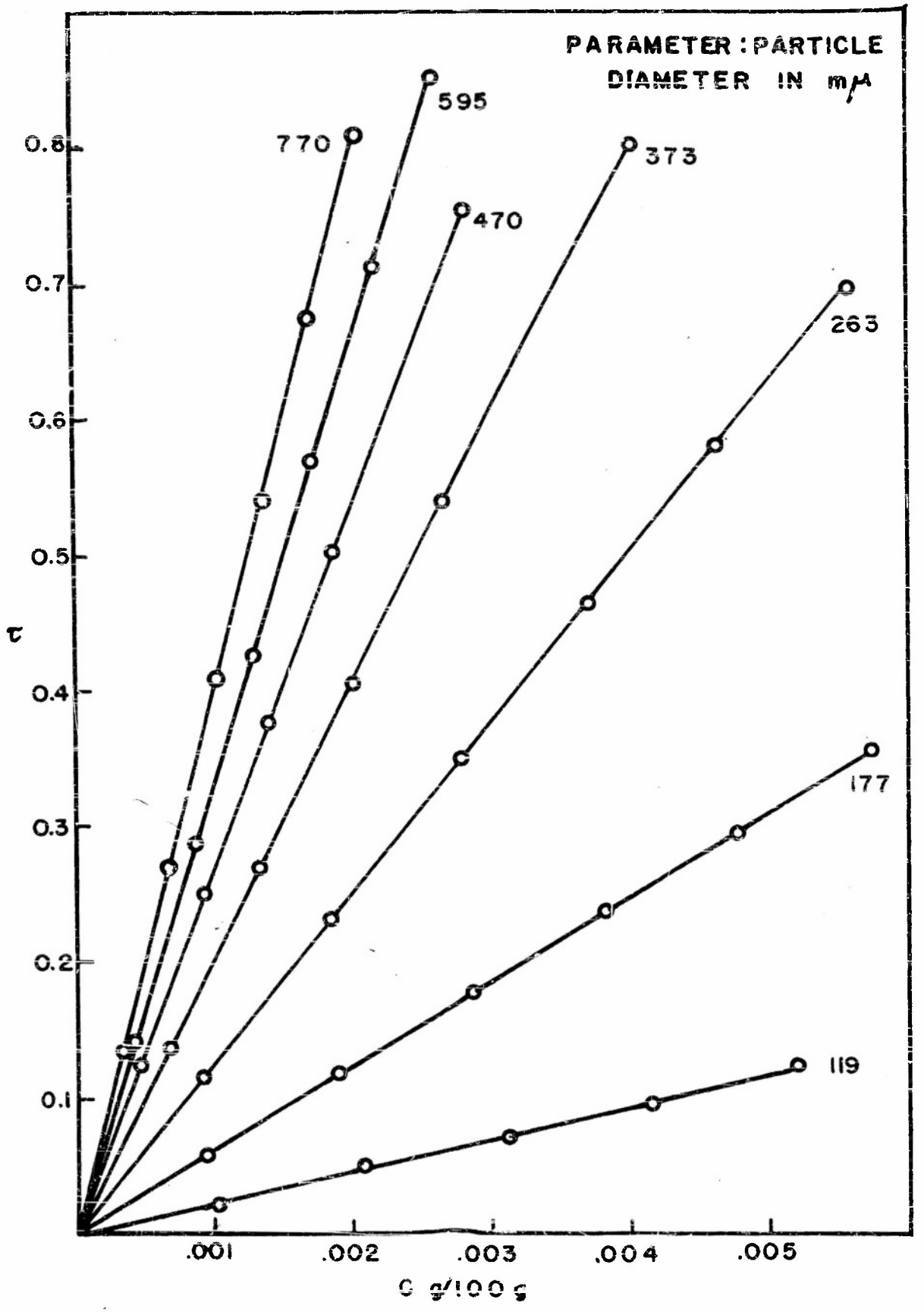

FIG. 10 TURBIDITY AS A FUNCTION OF CONC.

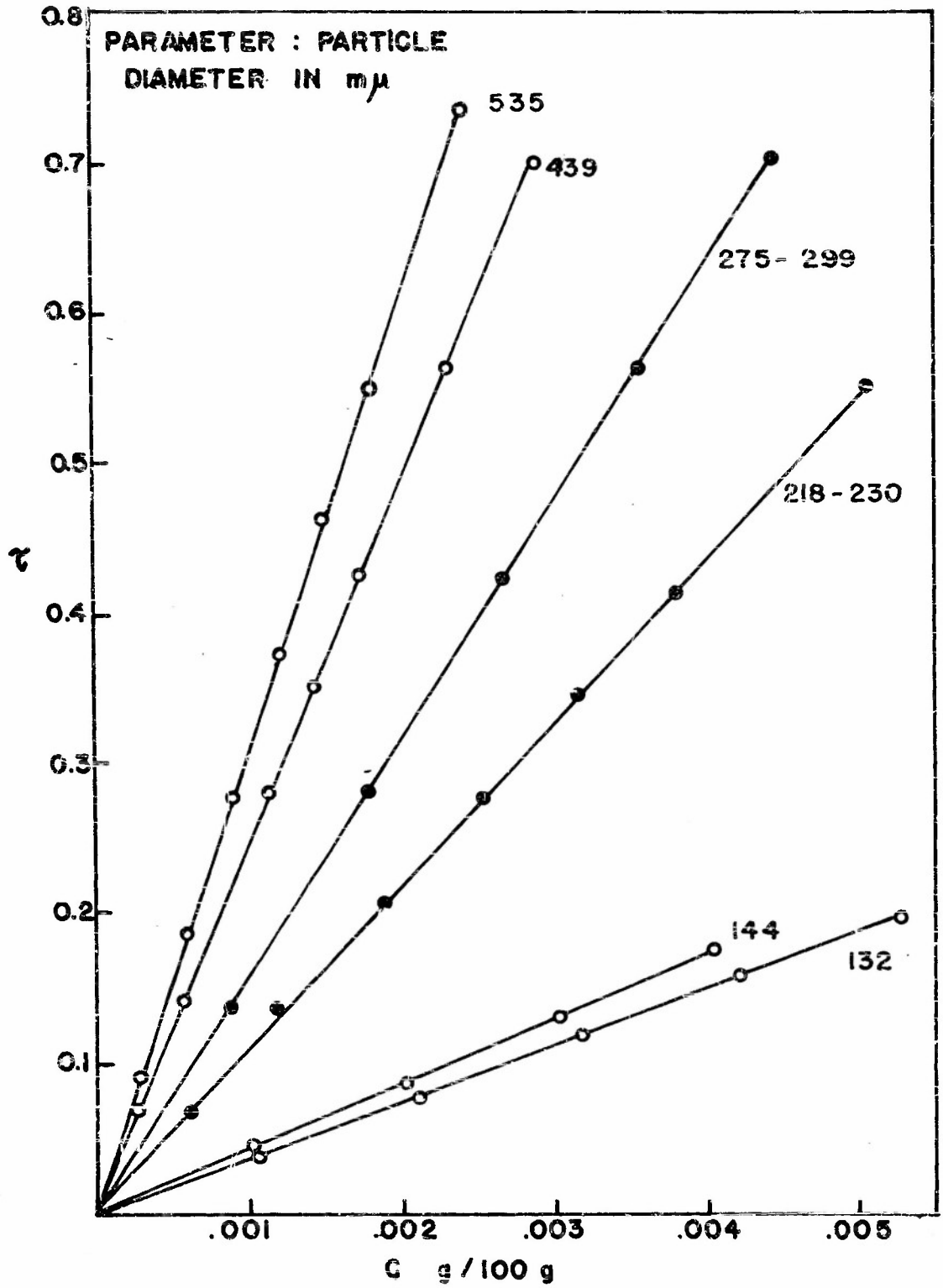

FIG. 11 TURBIDITY AS A FUNCTION OF CONC.

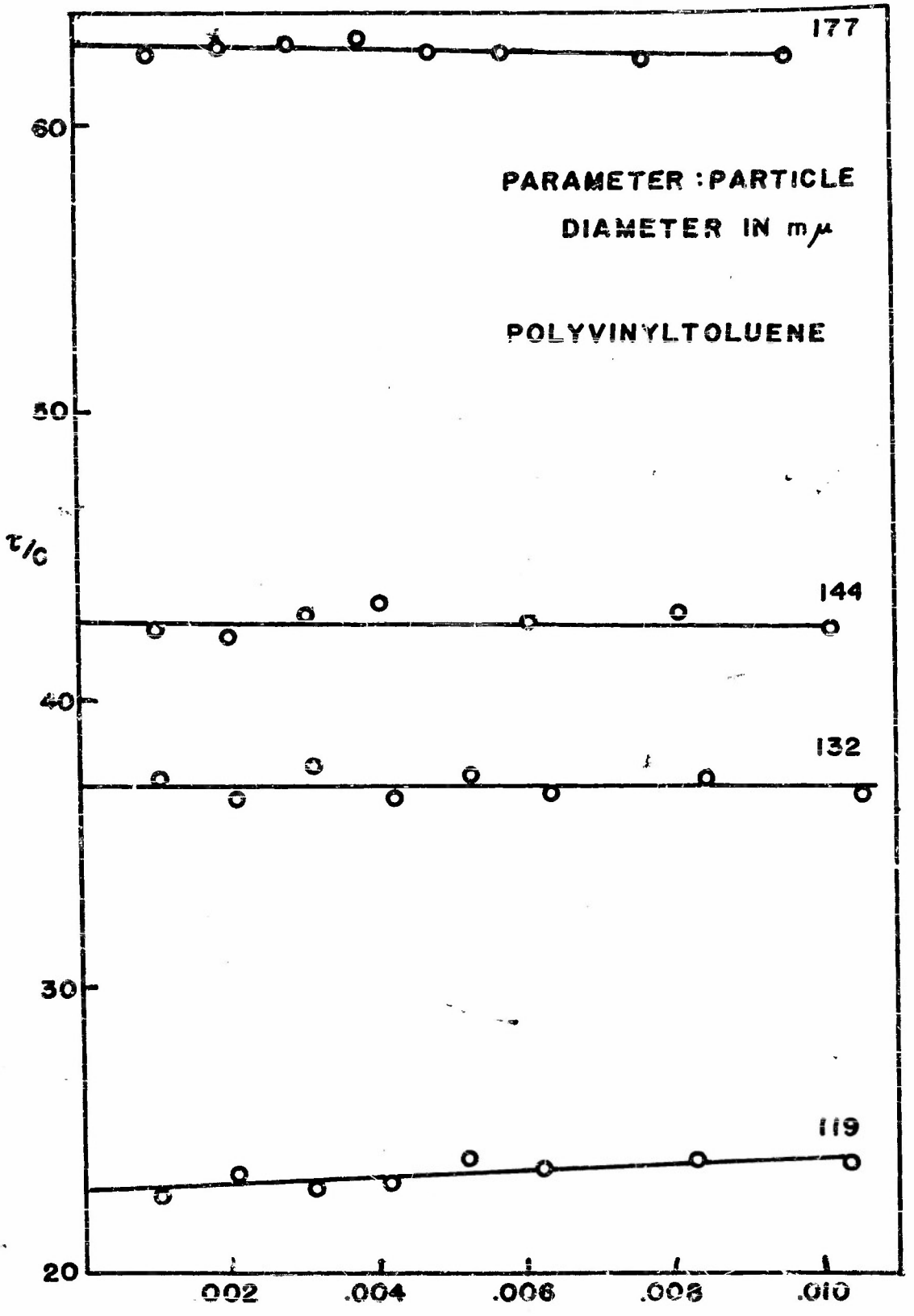

FIG. 12 SPECIFIC TURBIDITY vs. CONC.

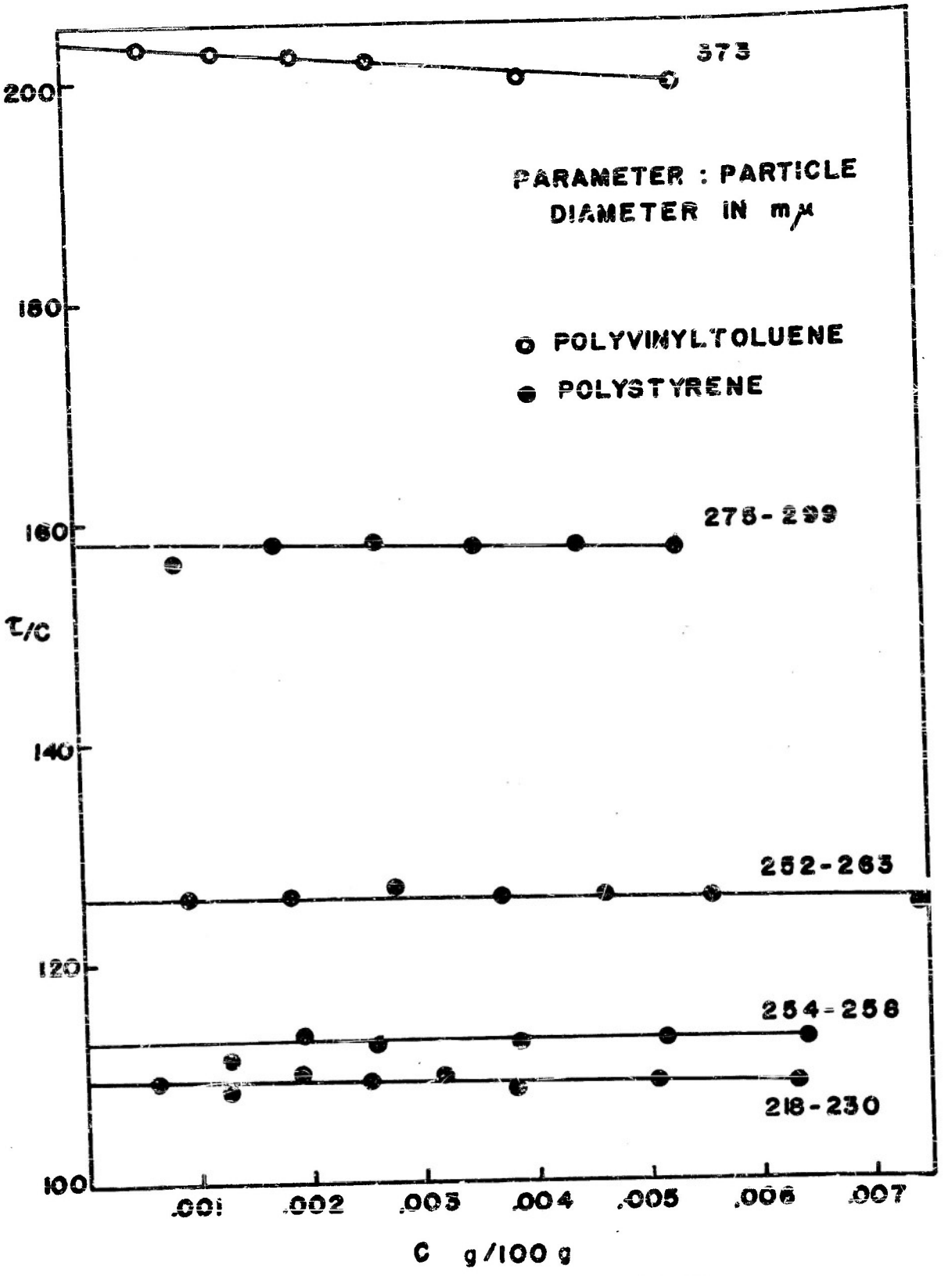

FIG. 13 SPECIFIC TURBIDITY vs. CONC.

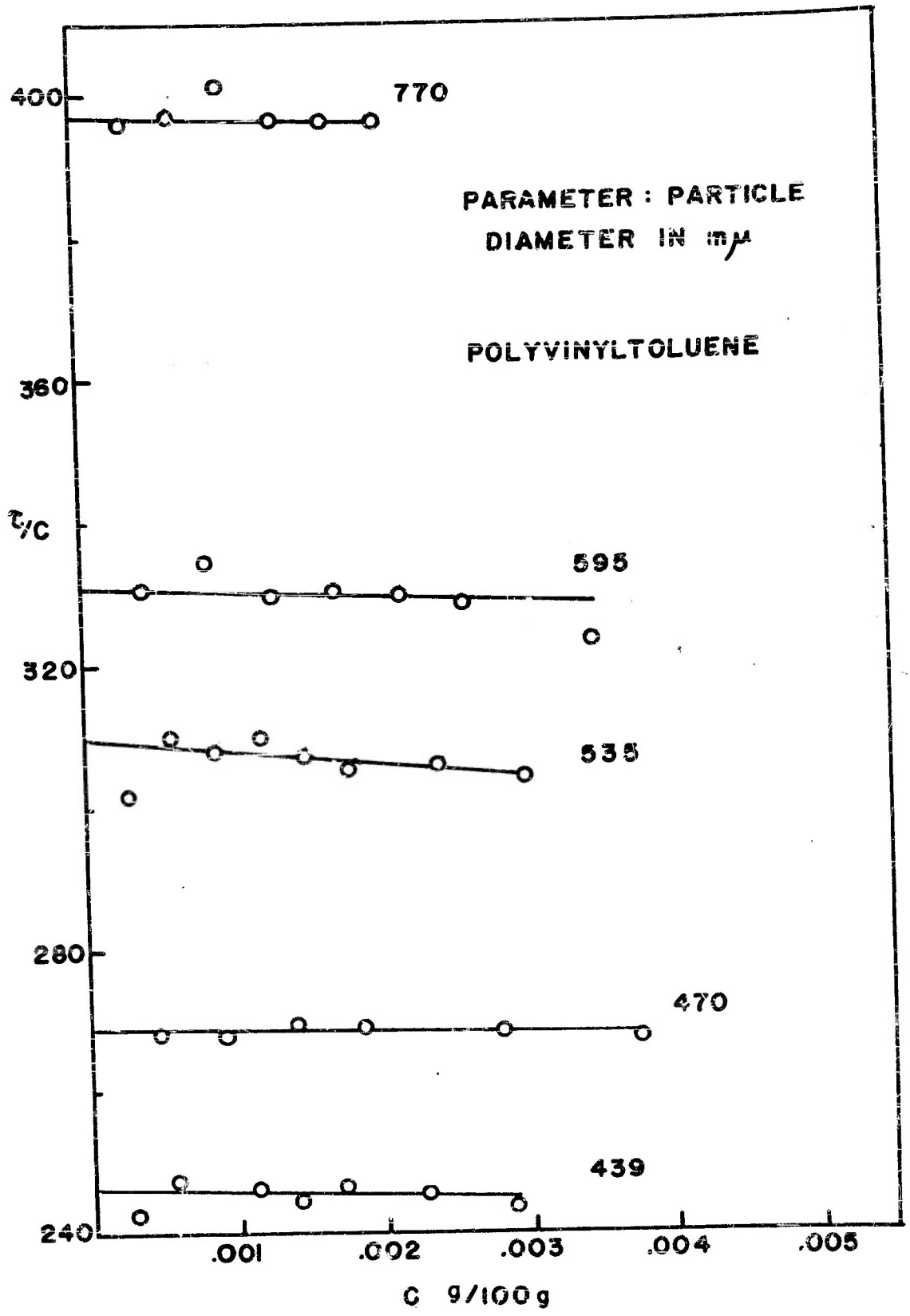

FIG. 14 SPECIFIC TURBIDITY vs. CONC.

FIG. 15

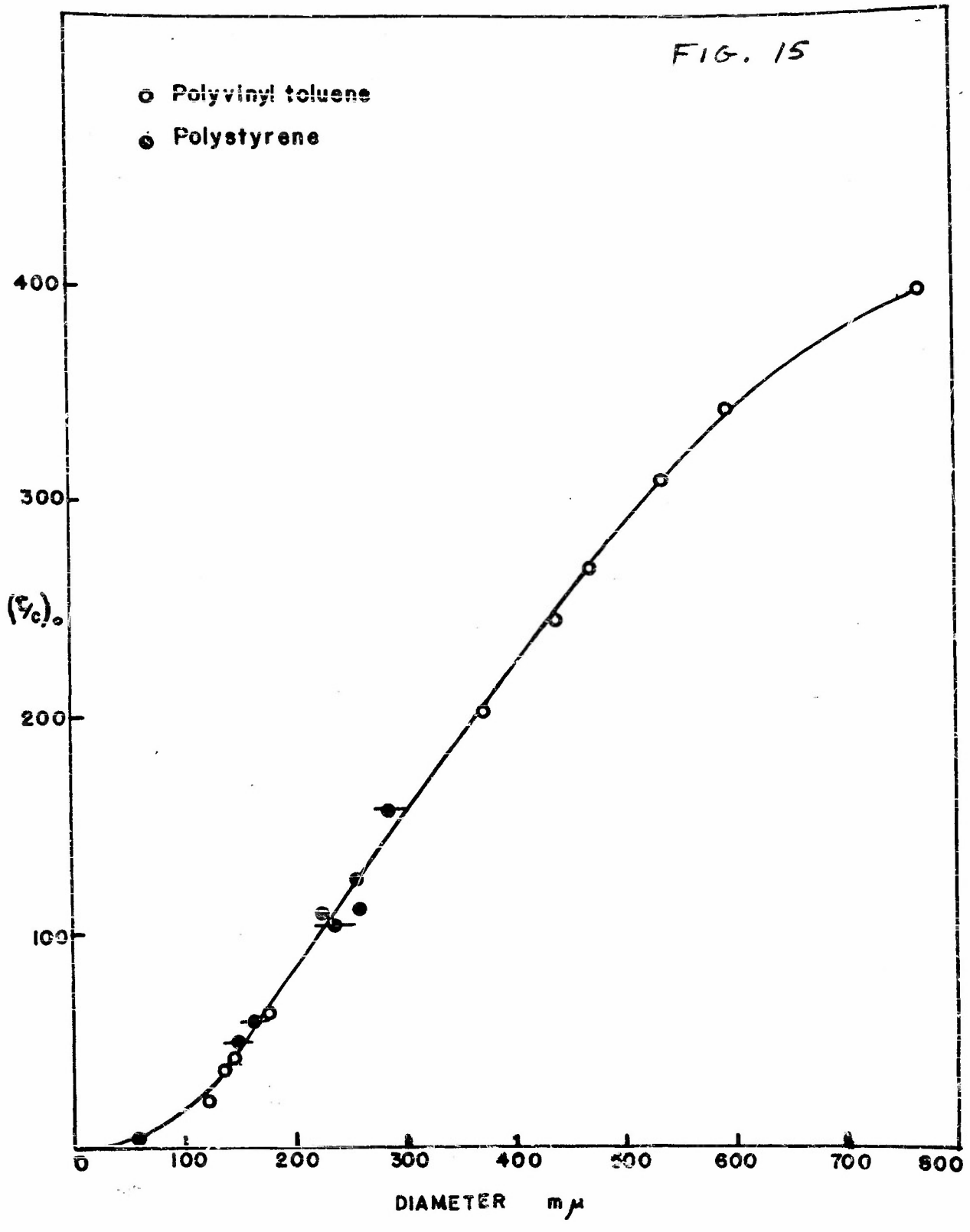
Polyvinyl toluene
Polystyrene
400
300
200
100
$(\tau_c)_o$
0
100
200
300
400
500
600
700
800
DIAMETER mμ

FIG 16

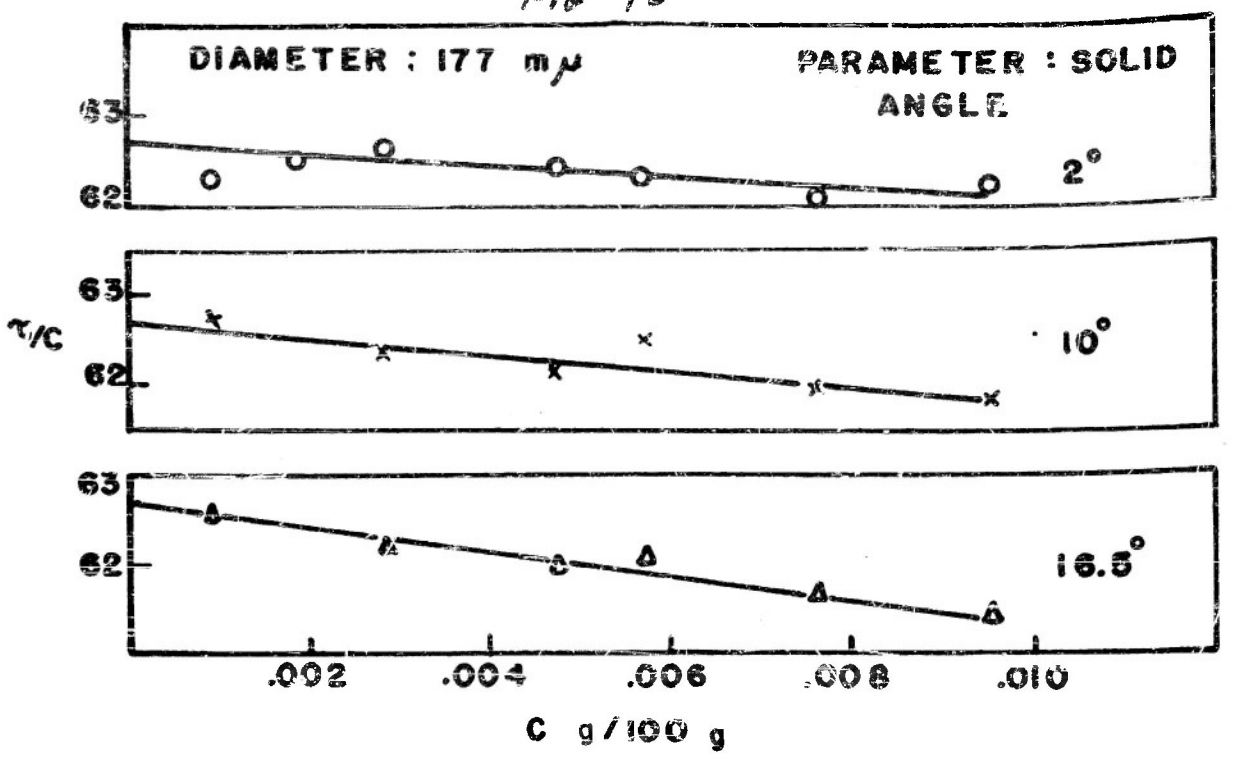
DIAMETER : 177 mμ
PARAMETER : SOLID ANGLE
63
62
2°
τ/C
63
62
10°
63
62
16.5°
.002
.004
.006
.008
.010
C g/100 g

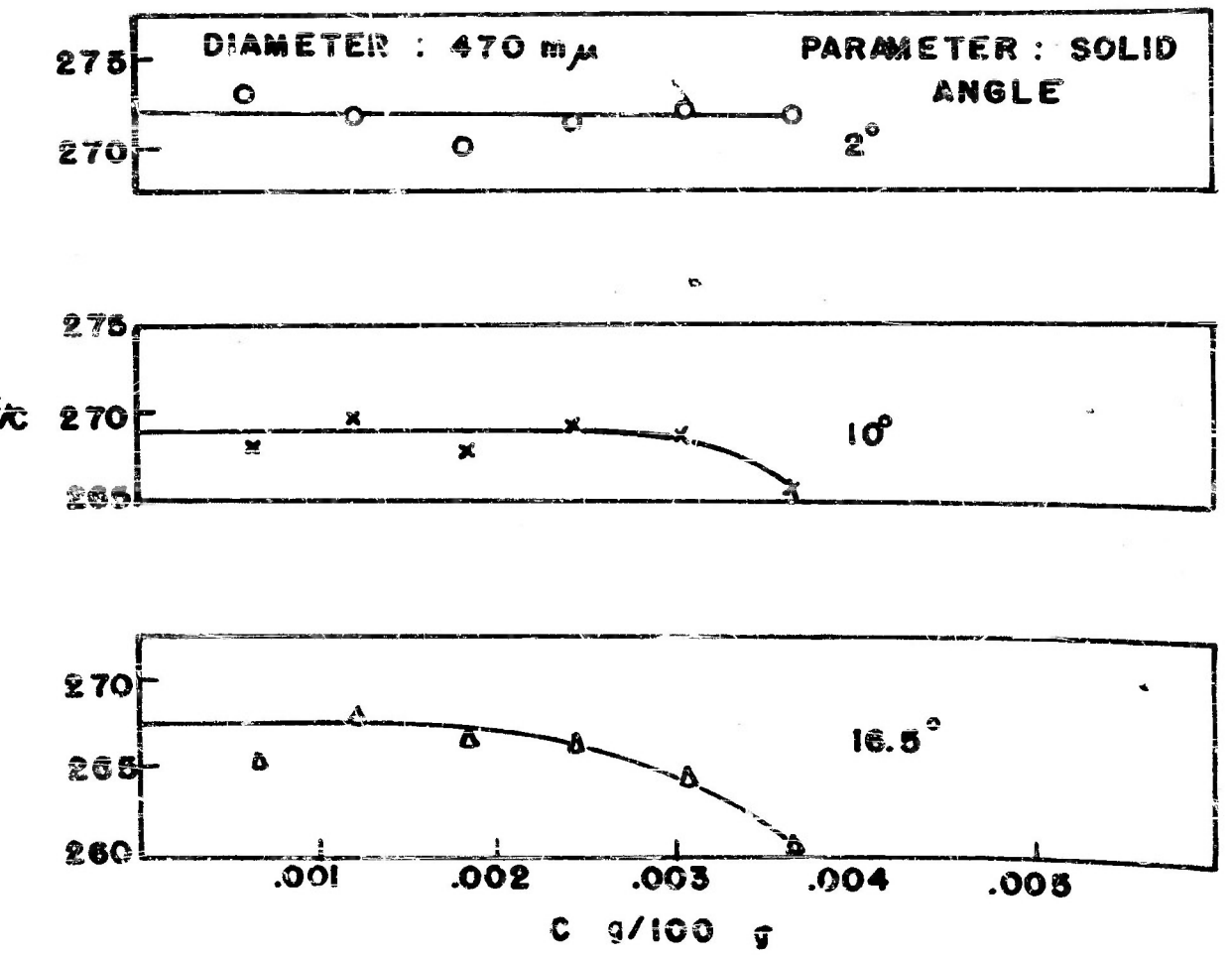
DIAMETER : 470 mμ
PARAMETER : SOLID ANGLE
275
270
2°
τ/C
275
270
10°
270
265
260
16.5°
.001
.002
.003
.004
.005
C g/100 g

FIG. 17

FIG. 18

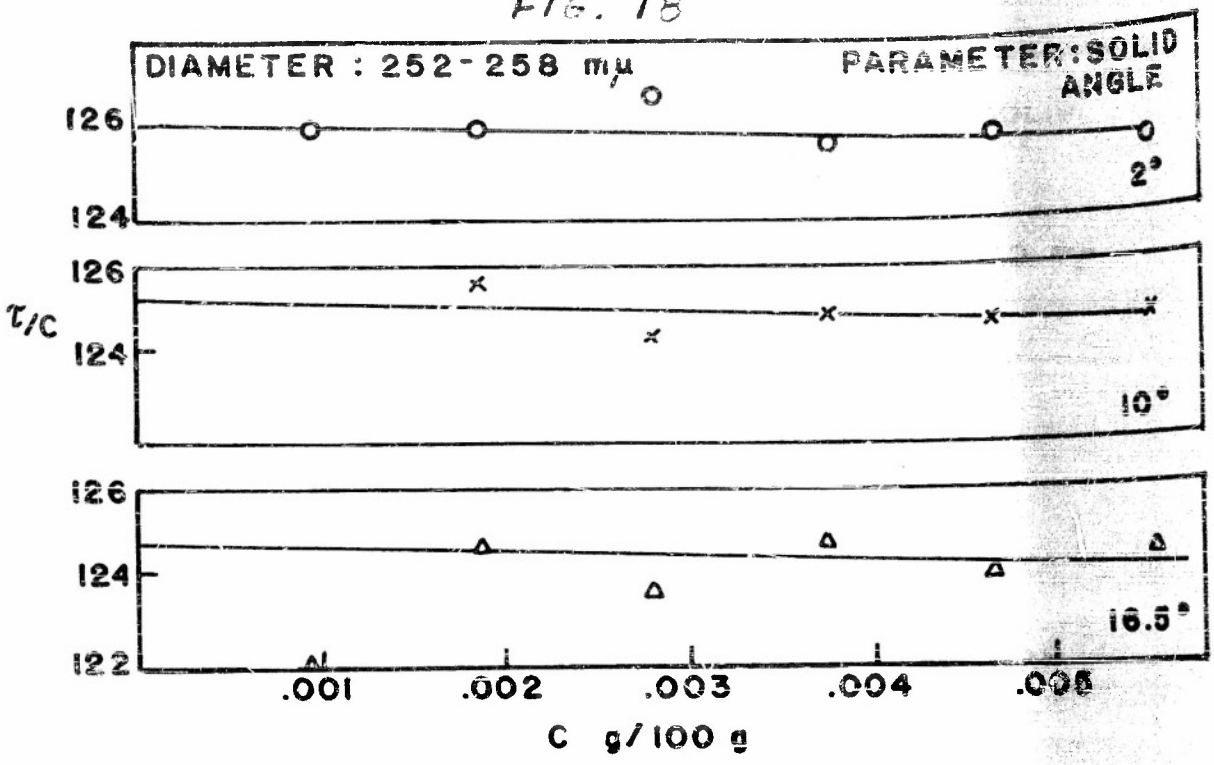
DIAMETER : 252-258 mμ
PARAMETER: SOLID ANGLE
2°
10°
16.5°
126
124
122
τ/C
.001
.002
.003
.004
.005
C g/100 g

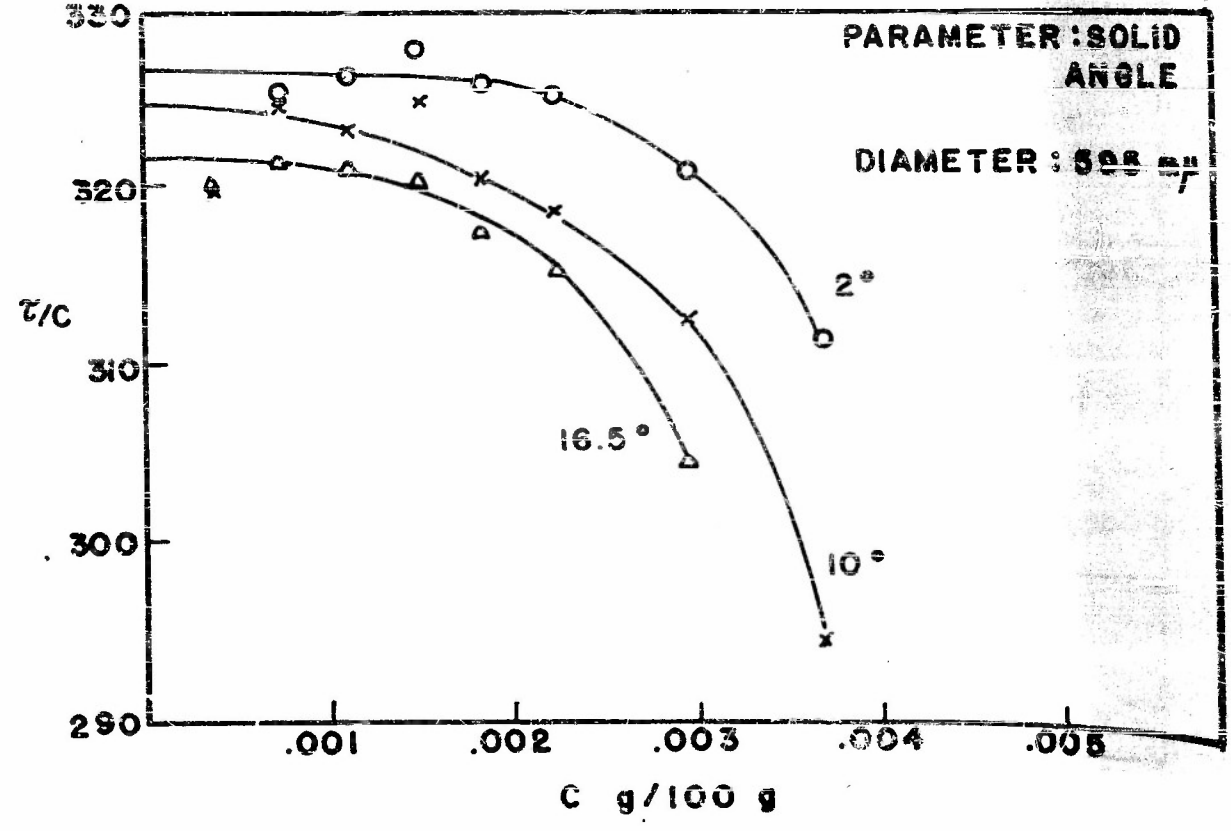
PARAMETER: SOLID ANGLE
DIAMETER : 508 mμ
2°
16.5°
10°
330
320
310
300
290
τ/C
.001
.002
.003
.004
.005
C g/100 g

FIG. 19

FIG. 18

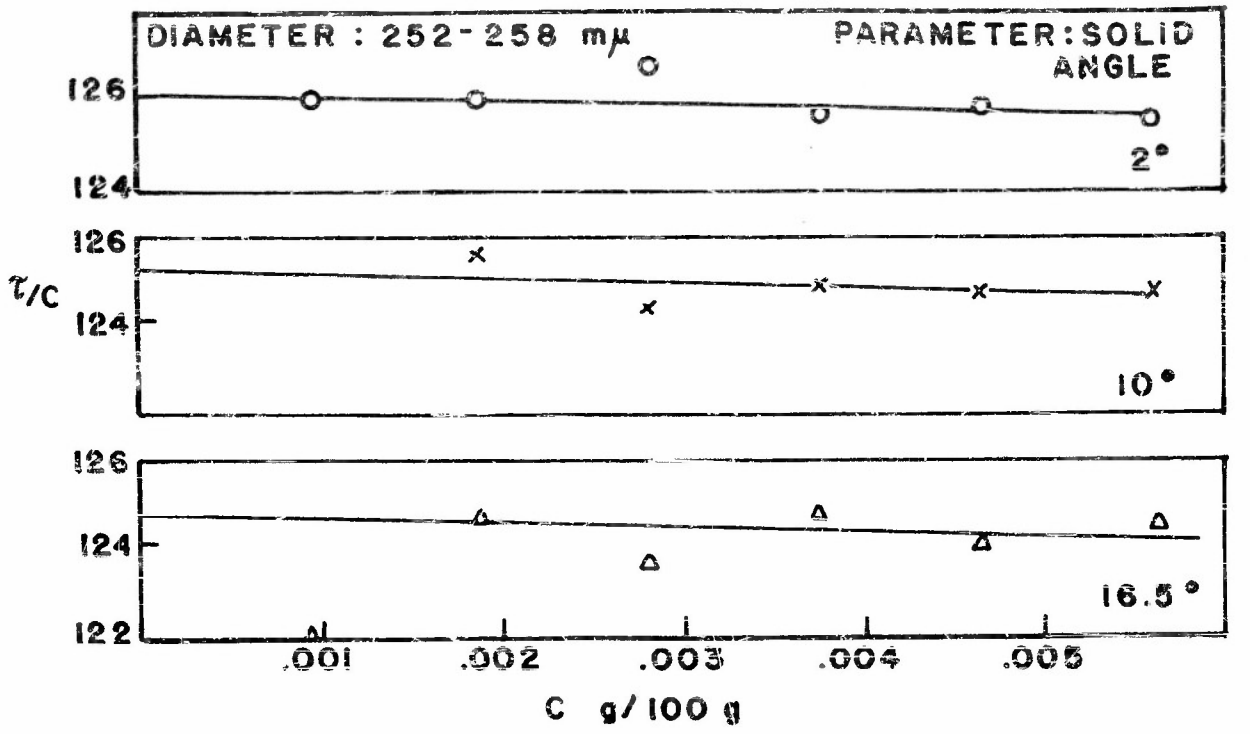
DIAMETER : 252-258 mμ
PARAMETER: SOLID ANGLE
126
124
2°
126
τ/C
124
10°
126
124
16.5°
122
.001
.002
.003
.004
.005
C g/100 g

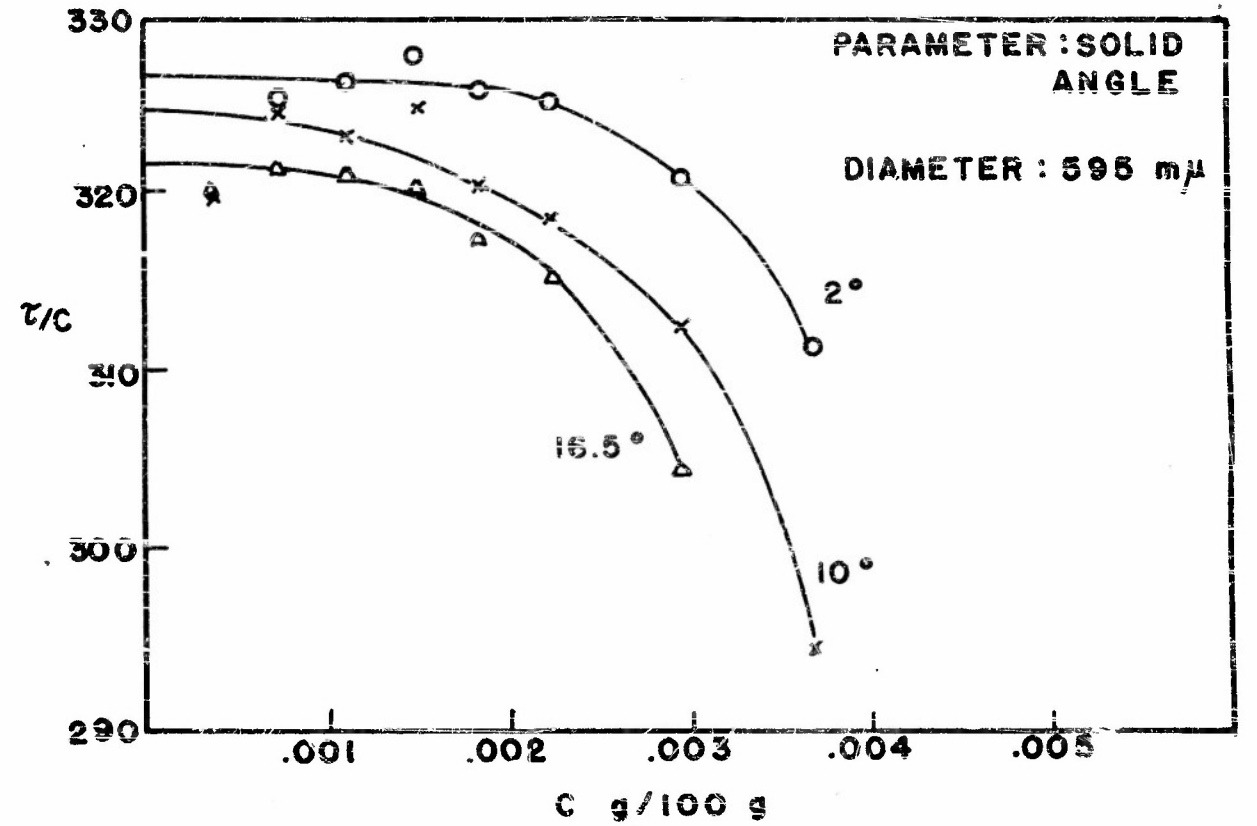
330
320
310
300
290
PARAMETER: SOLID ANGLE
DIAMETER : 595 mμ
τ/C
2°
16.5°
10°
.001
.002
.003
.004
.005
C g/100 g

FIG. 19

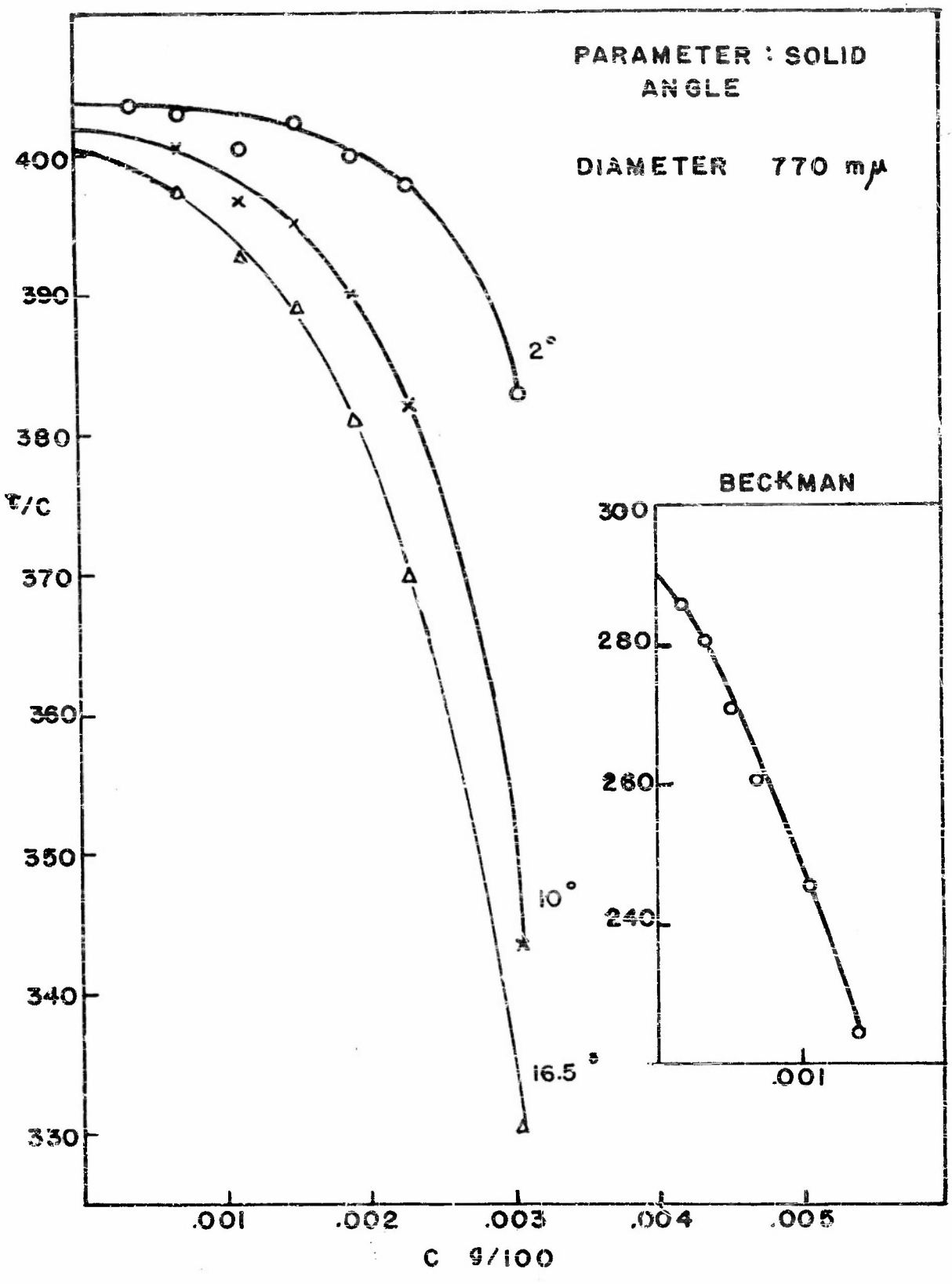
PARAMETER : SOLID ANGLE
DIAMETER 770 mμ
2°
10°
16.5°
BECKMAN
400
390
380
370
360
350
340
330
T/C
300
280
260
240
.001
.001
.002
.003
.004
.005
C g/100

FIG. 20

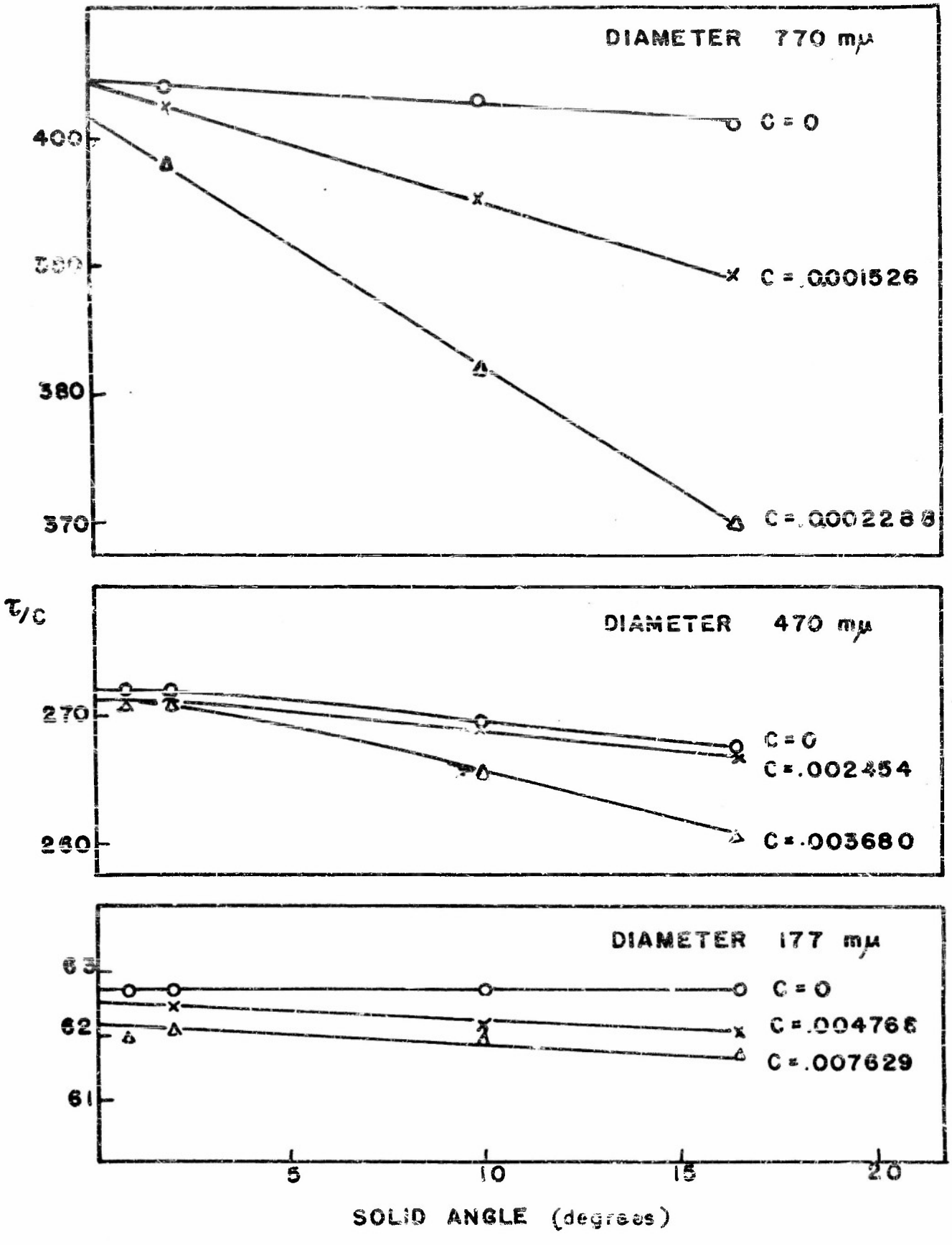
DIAMETER 770 mμ
C = 0
C = .0001526
C = .0002288
400
390
380
370
τ/c
DIAMETER 470 mμ
C = 0
C = .002454
C = .003680
270
260
DIAMETER 177 mμ
C = 0
C = .004766
C = .007629
63
62
61
5
10
15
20
SOLID ANGLE (degrees)

FIG. 21

FIG. 22

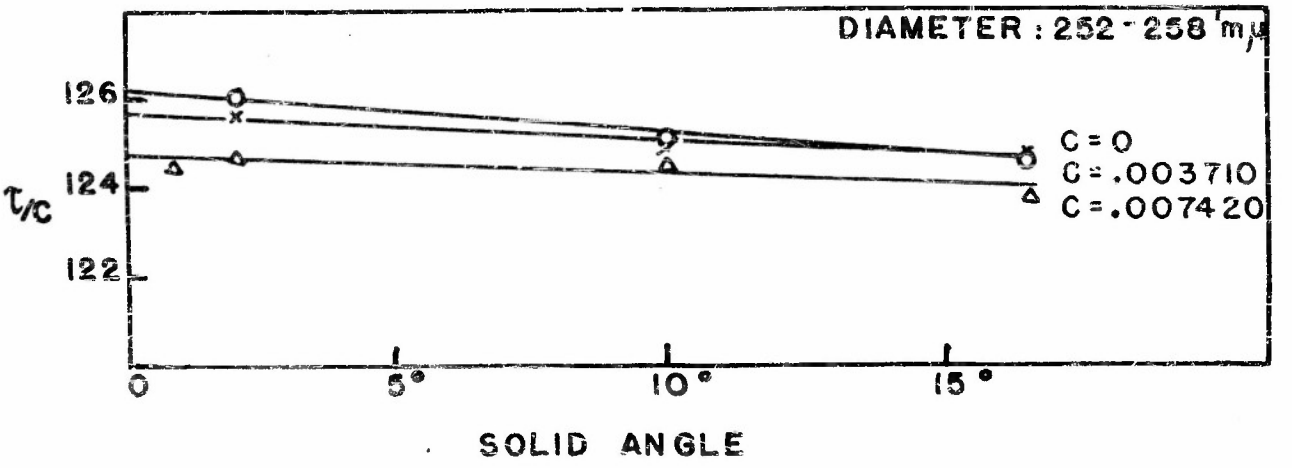
DIAMETER : 252 - 258 mμ
126
124
122
τ/c
C = 0
C = .003710
C = .007420
0
5°
10°
15°
SOLID ANGLE

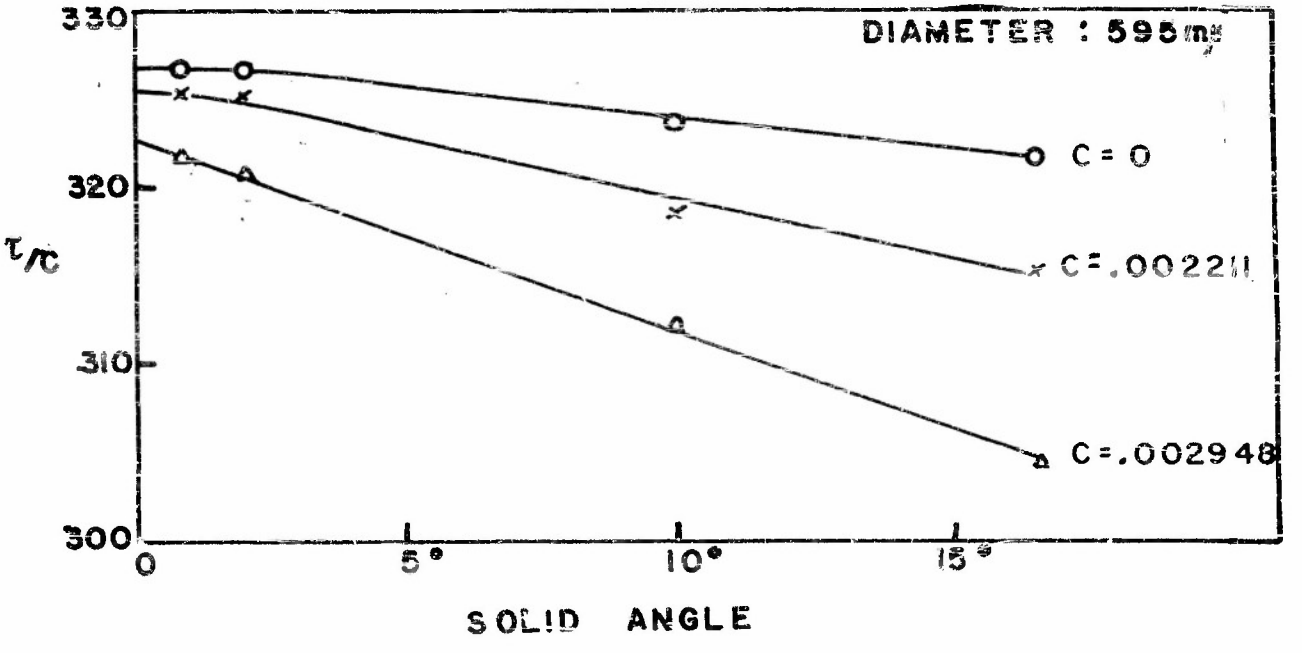
DIAMETER : 595 mμ
330
320
310
300
τ/c
C = 0
C = .002211
C = .002948
0
5°
10°
15°
SOLID ANGLE

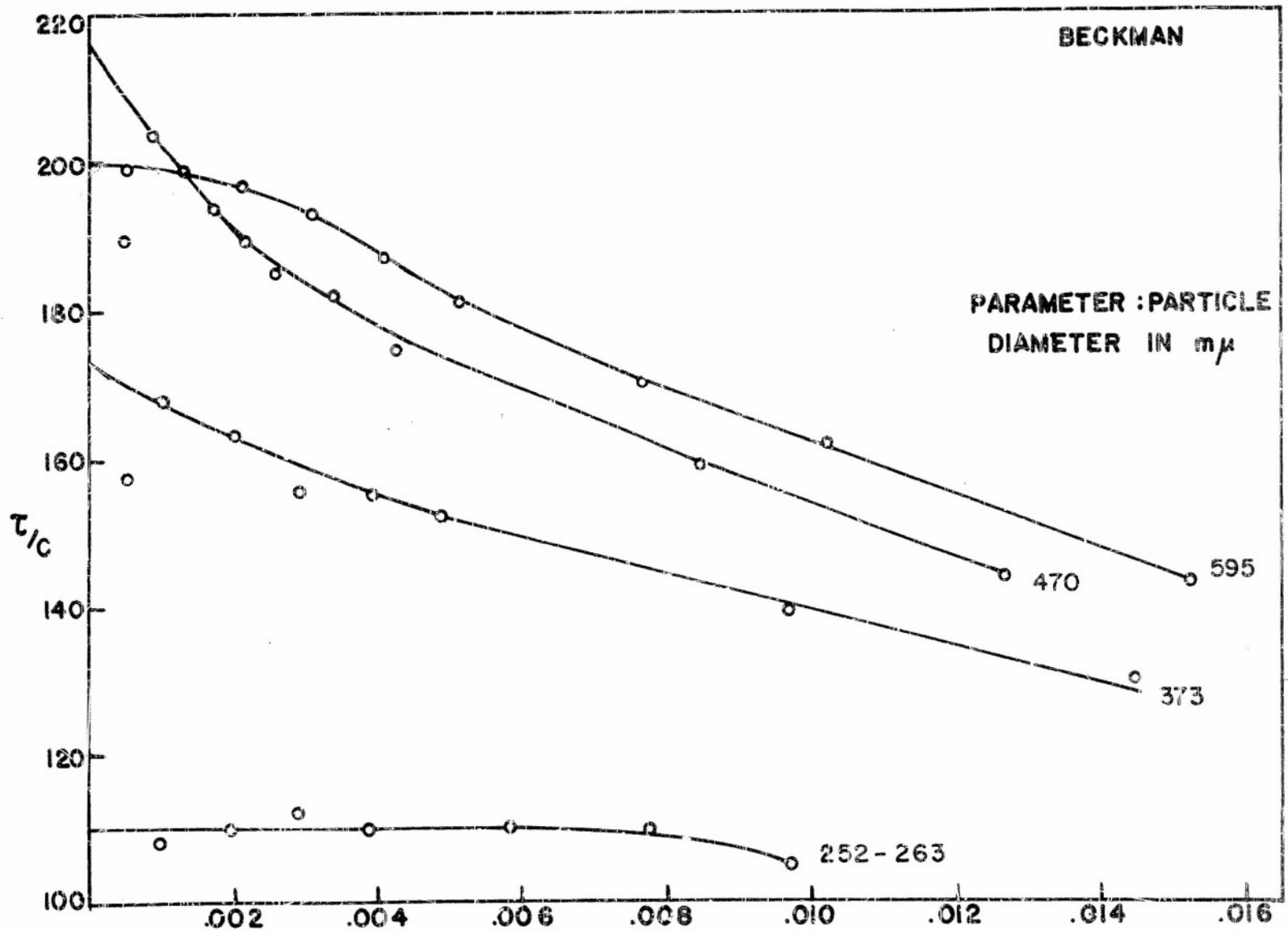

FIG. 23 SPECIFIC TURBIDITY vs. CONC.

FIG 24

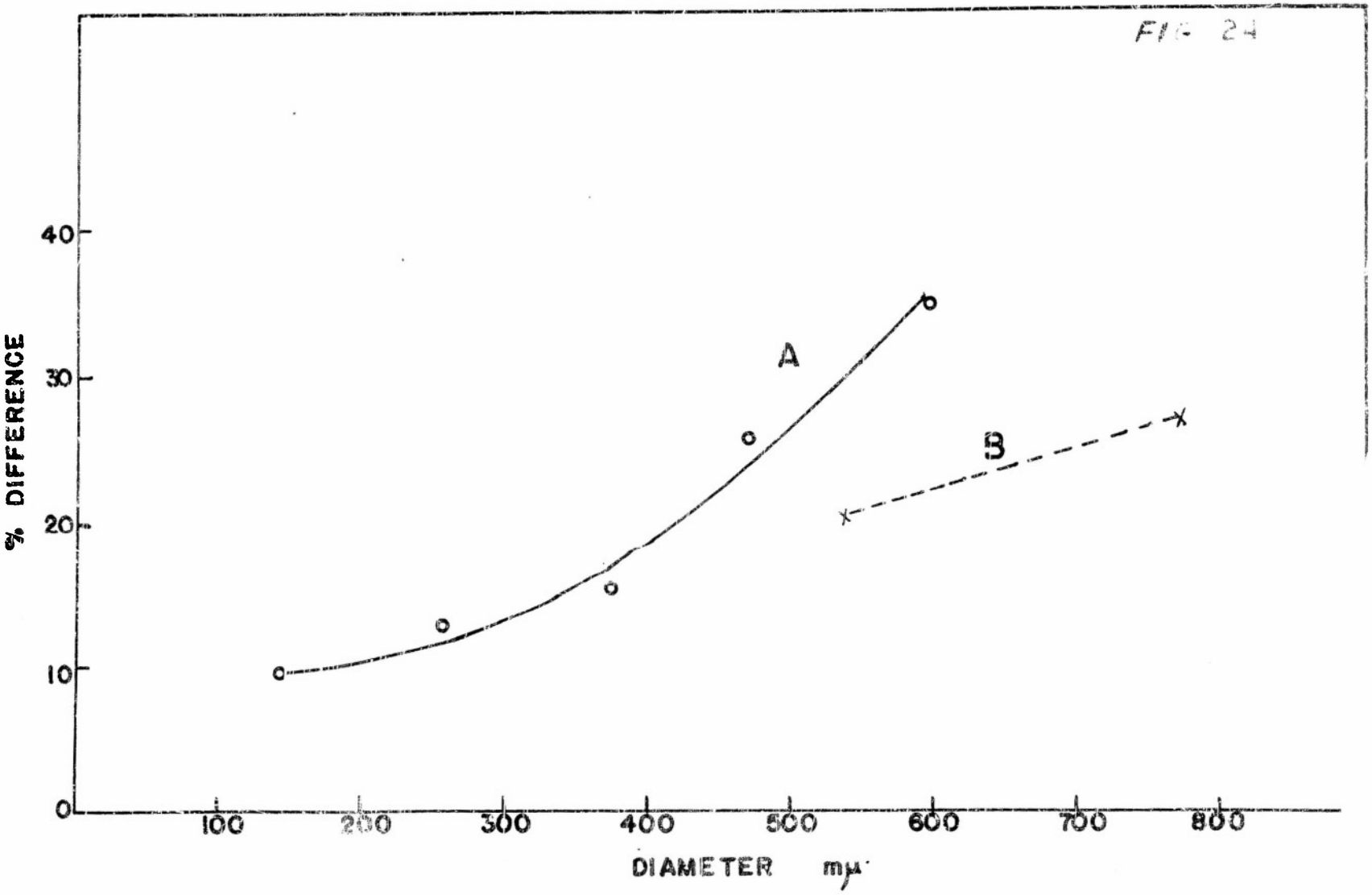
% DIFFERENCE
0
10
20
30
40
100
200
300
400
500
600
700
800
DIAMETER mμ
A
B